7 The Biogeochemistry of Iron

RALF R. HAESE

7.1 Introduction

For our understanding of interactions between living organisms and the solid earth it is fascinating to investigate the reactivity of iron at the interface of the bio- and geosphere. Similar to manganese (chapter 11) iron occurs in two valence states as oxidized ferric iron, Fe(III), and reduced ferrous iron, Fe(II). Two principal biological processes are of importance: Microorganisms such as magnetotactic bacteria and phytoplankton (see chapter 2 and section 7.3) depend on the uptake of iron as a prerequisite for their cell growth (assimilation). Others conserve energy from the reduction of Fe(III) to maintain their metabolic activity (dissimilation). In this case ferric iron serves as an electron acceptor which is also termed oxidant. Apart from biotic reactions manifold abiotic reactions occur depending on thermodynamic and kinetic conditions. Due to redox-reactions dissolution and precipitation of iron-bearing minerals may result which has great influence on the sorption/desorption and co-precipitation/release behavior of various components such as phosphate and trace metals. From a geologic point of view it is striking to find discrete iron enriched layers such as black shales or strata of the banded iron formation, which challenge geochemists to reconstruct the environmental conditions of their formation.

7.2 Pathways of Iron Input to Marine Sediments

Within the continental crust iron is the fourth most abundant element with a concentration of 4.32 wt% (Wedepohl 1995). It is transported to marine sediments by four major regimes: fluvial, aeolian, submarine hydrothermal, and glacial input. For the investigation of iron reactivity it is important to differentiate regions of predominant input regimes since characteristic reactions occur at the interface of the transport regime and the marine environment. For the chemistry of hydrothermal fluids and reactions during mixing with seawater refer to chapter 13.

7.2.1 Fluvial Input

In Figure 7.1 averaged concentrations of dissolved and particulate iron, major fluxes and the respective predominant reactions are shown. Dissolved iron concentrations in averaged river and marine water clearly show less solubility in marine relative to river water. In contrast, the concentration of particulate iron does not change significantly and is similar to the average continental crust concentration. This is also reflected in the conservative behavior of iron under chemical weathering conditions. Along with Al, Ti and Mn, Fe belongs to the refractive elements (Canfield 1997). Note that in Fig. 7.1 the given value for particulate iron concentration in marine sediments is derived from pelagic clay sediments. Biogenic constituents such as carbonate and opal may significantly dilute the terrigineous fraction (chapter 1) and thus decrease the iron concentration.

The decrease of dissolved iron concentrations can be traced within estuarine mixing zones. Within river water, dissolved iron is mainly present as Fe(III)oxyhydroxide, which is stabilized in colloidal dispersion by high-molecular-weight humic acids (Hunter 1983). Due to increasing salinity and thus increasing ionic strength the colloidal dispersion becomes electrostatically and chemically destabilized which results in the coagulation of the fluvial colloids. This process is reflected in Fig. 7.2 showing dissolved iron along a transect off the mouth of the Congo (formerly: Zaire) river

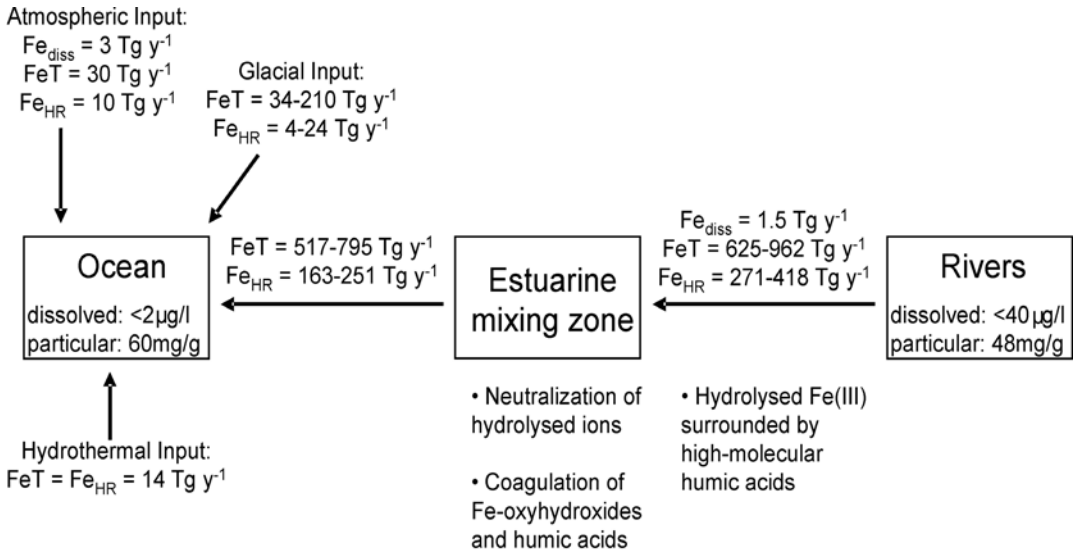

Fig. 7.1 Global fluxes of dissolved (Fe_{diss}), highly reactive iron (FeHR) and total iron (FeT) from riverine, glacial, atmospheric and hydrothermal sources. The estuarine mixing zone serves as a major sink for dissolved and highly reactive (dithionite-soluble) iron. Fluxes and concentrations are given according to Poulton and Raiswell (2002). The atmospheric dissolved iron flux was taken from Duce et al. (1991).

towards the open ocean. With increasing salinity the concentration of dissolved iron decreases exponentially. These results also point out the operatively defined differentiation of dissolved and particulate phase. The concentration of dissolved iron depends on the pore size of the used filters. Commonly, particles smaller than 0.4 µm are considered to be 'dissolved'.

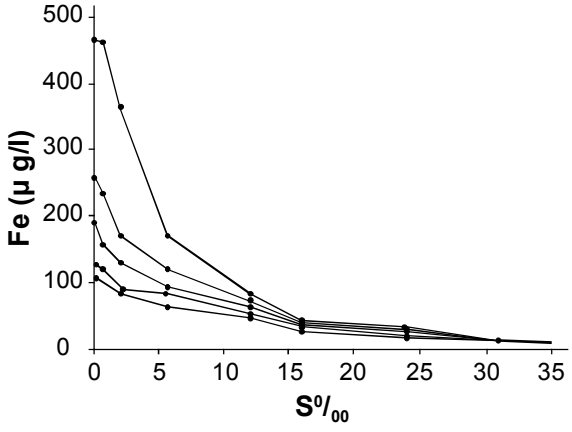

Fig. 7.2 Dissolved iron concentrations of surface water from a transect off the Congo River towards the open ocean. Pore sizes of 1.2, 0.45, 0.22, 0.05 and 0.025 µm (according to graphs from above downward) were used to separate particulate from dissolved phase (adopted from Figuères et al. 1978).

Apart from being a zone of coagulation the estuarine and coastal zone represents the most important sink for dissolved and particulate iron of fluvial origin. A recent study by Poulton and Raiswell (2002) provides quantitative evidence for the important role of estuaries for iron transformations at the Earth's surface (Fig. 7.1): The high degree of chemical weathering in the catchments of rivers discharging into the global ocean leads to a high proportion of highly reactive iron ($Fe_{HR,dithionite\ soluble}$) relative to total iron (FeT), with Fe_{HR}/FeT = 0.43. In contrast, glaciers discharge sediments which were formed predominantly under physical weathering conditions and reveal a mean Fe_{HR}/FeT of 0.11. Approximately 40 % of the riverine highly reactive iron fraction is retained in the estuarine and near-coastal zone, which, together with the low Fe_{HR} proportion in glacial sediments leads to a Fe_{HR}/FeT of 0.26 in marine sediments. The iron inputs from atmospheric and hydrothermal sources are relatively small, i.e. less than 10 % of Fe_{HR} and FeT as compared to the riverine input (Fig. 7.1).

7.2.2 Aeolian Input

In contrast to the fluvial transport regime the aeolian transport is highly efficient for the deposition of terrigenous matter in the deep sea.

Donaghay et al. (1991) published a global map of atmospheric iron flux to the ocean (Fig. 7.3). Among others the North African desert and Asia can be identified as major dust sources. Asian loess is transported across the northern Pacific making up to 100 % of the terrigenous fraction of pelagic sediments (Blank et al., 1985) and North African dust is spread out over the north equatorial Atlantic eventually reaching the Caribbean Sea (Carlson and Prospero 1972) and the northern coast of Brazil (Prospero et al., 1981). Iron settles out of wind-driven air layers by wet deposition which can be traced in equatorial areas (Murray and Leinen 1993) where a distinctively high humidity occurs within the Inner Tropical Convergence Zone (ITCZ). Therefore, a characteristic high deposition of iron occurs at the equatorial Atlantic (Fig. 7.3).

As iron is discussed as limiting nutrient for phytoplankton productivity of distinct oceanic regions (chapter 7.3) it is important to investigate the flux, degree of solubility and the bioavailability of the introduced iron into open ocean surface water. It has long been known that sorption onto suspended particles is highly efficient in the removal of trace metals from solution (Krauskopf 1956) resulting in a decrease of dissolved concentration relative to the thermodynamic saturated concentration. Chester (1990) listed the solubility of several trace metals in coastal and open ocean surface water and specified the solubility of aeolian transported iron with ≤ 7 %. This is in agreement with a short review of published results provided by Zhuang et al. (1990) revealing a range of iron solubility between 1 and 10 %. By contrast, Zhuang et al. (1990) themselves found a solubility of ~50 % of atmospheric iron suggesting that all the dissolved iron in North Pacific surface water is provided by atmospheric input. Zhuang and Duce (1993) could show that the concentration of suspended particles is the prime variable controlling the adsorbed fraction, yet, an increase in aeolian deposition would also result in an increase of net dissolved iron.

The reason for the dissolution of solid phase iron in the photic zone is the photochemical reduction of Fe(III), with UVB (280 – 315 nm) producing most of Fe(II), followed by UVA (315 – 400 nm) and visible light (400 – 700 nm) (Rijkenberg et al. 2005). As a consequence, about 10 % of atmospheric FeT reaches the ocean as dissolved iron (Duce et al. 1991; Fig. 7.1). In surface waters of the global ocean the produced Fe^{2+} is subsequently reoxidized, yet, the photoreduction

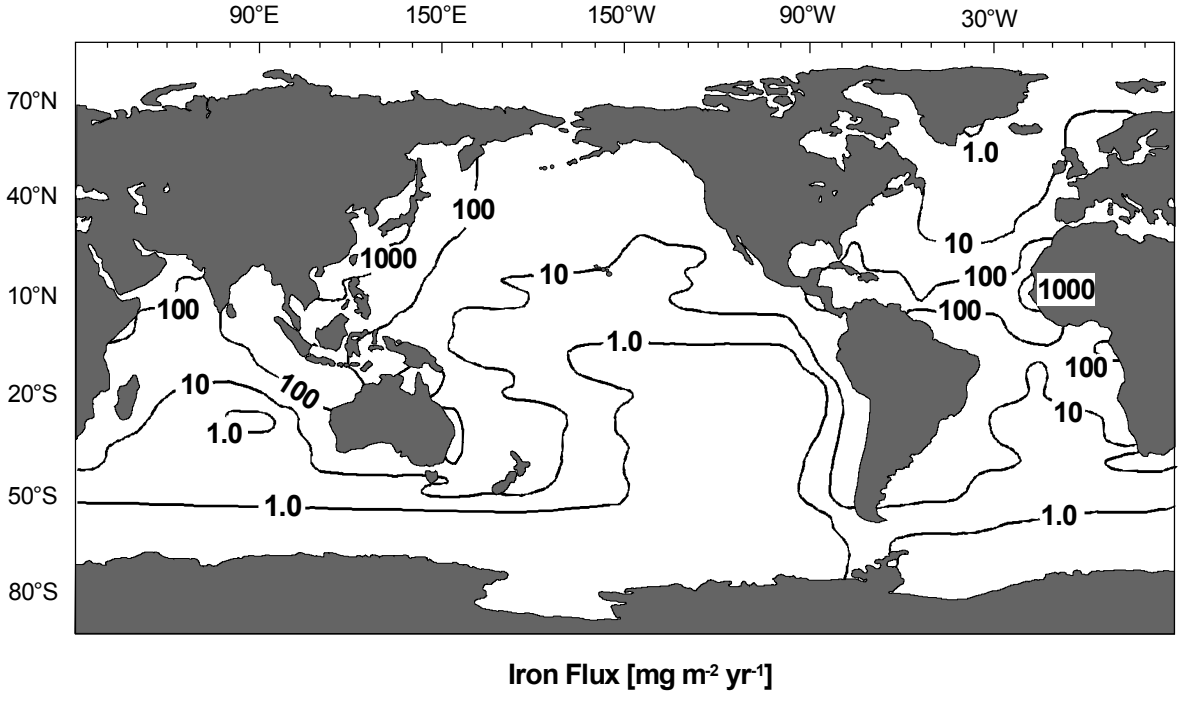

Fig. 7.3 Global map of atmospheric iron fluxes to the deep sea (adopted from Donaghay et al. 1991).

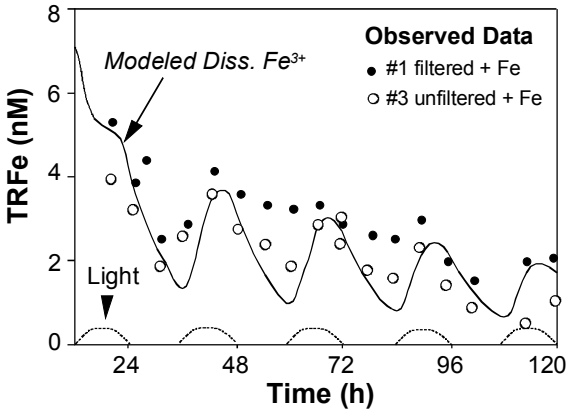

Fig. 7.4 Measured iron concentrations in incubations (dots) and model (solid line) results of dissolved iron within surface ocean water. The artificial light intensity (dashed line) drives the photochemical reduction. The gradual decrease of dissolved iron is caused by the uptake by phytoplankton (adopted from Johnson et al. 1994).

causes a net increase of dissolved iron. Model and experimental results by Johnson et al. (1994) reflect the dependence of dissolved iron on irradiation (Fig. 7.4). During incubations diurnal cycles and gradually decreasing dissolved iron concentrations result from induced daily irradiation and a gradual uptake by phytoplankton.

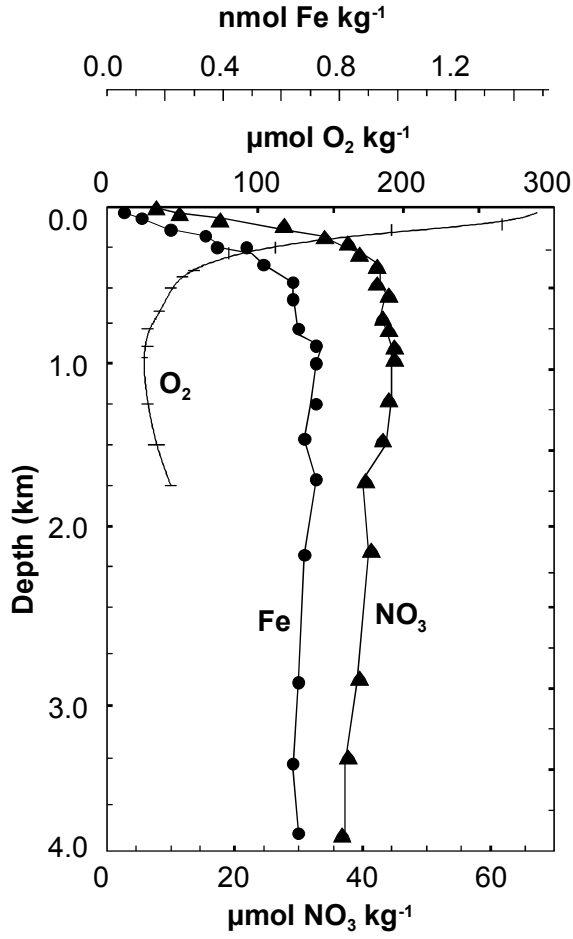

Fig. 7.5 Vertical distribution of NO_3^-, dissolved iron and oxygen at a station of the Gulf of Alaska (adopted from Martin et al. 1989).

7.3 Iron as a Limiting Nutrient for Primary Productivity

The growth of phytoplankton in the world ocean is undoubtedly one of the driving influences for the global carbon cycle and thus for the present and past climate (Berger et al. 1989; de Baar and Suess 1993). This primary productivity (PP) is limited by the availability of nutrients. Apart from the major nutrients nitrogen, phosphorous and silica so called micronutrients - especially iron - have long been speculated to have a limiting control on PP (Hart 1934). Yet, detailed investigations concerning their importance for the carbon cycle have only been possible for the past ten years due to analytical reasons. Virtually all microorganisms require iron for their respiratory pigments, proteins and many enzymes. Therefore, dissolved iron shows a similar vertical profile in the water column as nitrate being reduced to near zero within the surface layer where PP takes place and being increased within the oxygen minimum zone due to the mineralization of iron bearing organic matter (Fig. 7.5).

Three major oceanic regions (20 % of the world's open ocean) are characterized by high-nitrate and low-chlorophyll (HNLC) concentrations. The PP of the Southern Ocean (Broecker et al., 1982), the equatorial Pacific (Chavez and Barber 1987) and the Gulf of Alaska (McAllister et al. 1960) are obviously not limited by nitrate. Alternatively, as atmospheric dust loads in the Antarctic and equatorial Pacific are the lowest in the world (Prospero 1981; Uematsu et al. 1983) the importance of iron as limiting micronutrient for PP became increasingly discussed.

The effect of added atmospheric dust to clean sea water from HNLC-regions were studied in

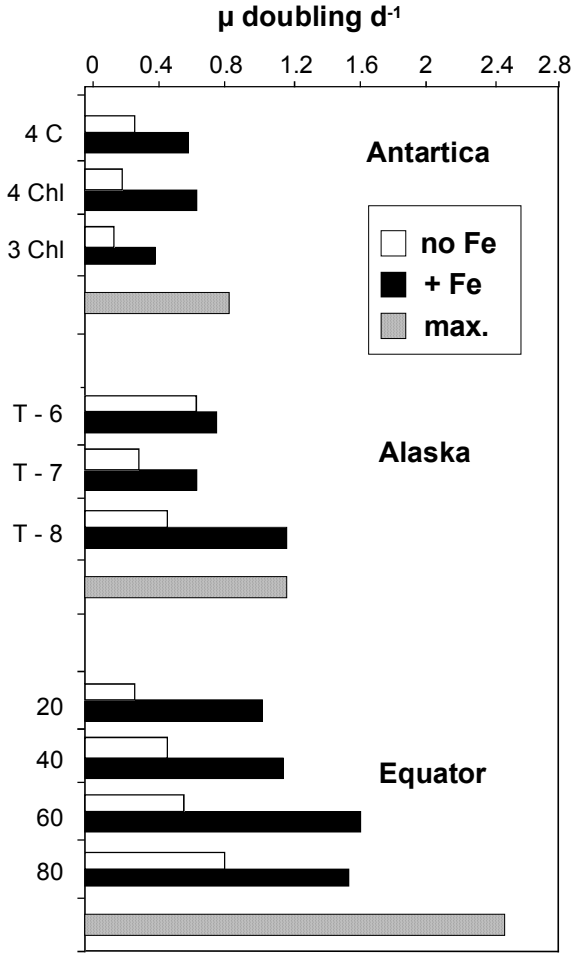

Fig. 7.6 The effect of iron addition to surface water of high-nutrient, low-chlorophyll (HNLC) regions. The doubling rate, μ, is an expression for the increase of primary productivity and maximum values, max., depend on light intensity and temperature. An increase of primary productivity by a factor of 2-4 is resulting due to the addition of atmospheric iron (adopted from Martin et al. 1991).

bottle experiments by Martin et al. (1991) demonstrating increased PP by a factor of 2-4 (Fig. 7.6). Since the role of large grazers living on phytoplankton was not considered by such experiments doubts and open questions to use these laboratory results for statements on large-scale environmental processes remained. Therefore, Martin and colleagues conducted a large-scale iron enrichment experiment south of the Galapagos Islands in the equatorial Pacific (Martin et al. 1994). A total volume of 15,600 l of iron solution (450 Kg Fe) were distributed by ship over an area of 64 km^2 which increased the original dissolved iron concentration of 0.06 nM to ~4 nM. Iron concentrations, various parameters monitoring primary productivity and an inert tracer were continuously analyzed for 10 days. As a result they did find an increase of PP by a factor of 2-4 within the iron fertilized open ocean patch (Martin et al. 1994) which gave evidence for the importance of iron as limiting micronutrient within HNLC-areas.

Compelling evidence for the limitation of phytoplankton productivity by the availability of dissolved iron was also found in surface waters of the Peru shelf by comparing the nutrient inventories of the northern, chlorophyll-rich, 'brown' waters to the southern, chlorophyll-poor, 'blue' waters (Bruland et al. 2005). Surface waters of both areas receive large fluxes of macronutrients through upwelling, but only the bottom waters of the northern area are suboxic and rich in dissolved iron (> 50 nM). The constant replenishment of dissolved iron from iron-rich bottom waters leads to very high primary productivity in the northern Peru shelf region whereas the southern region is characterized by high (macro-) nutrient and low chlorophyll concentrations.

If iron is a limiting micronutrient for present-day PP, it may be an important link to explain glacial-interglacial climatic cycles of the past. Martin (1990) postulated the 'iron hypothesis' which explains decreased atmospheric CO_2 concentrations during glacial times with increased iron deposition by aeolian input resulting in increased PP and thus increased CO_2-

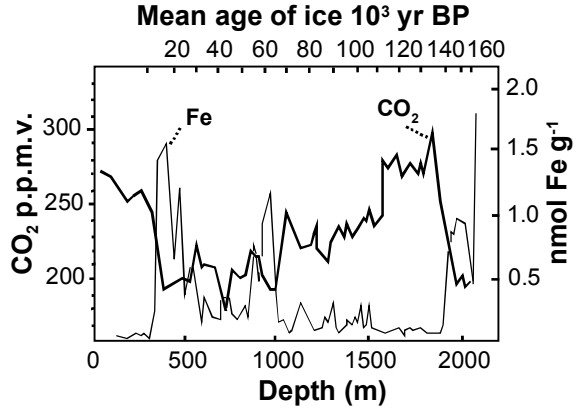

Fig. 7.7 Fe and CO_2 concentrations of the Antarctic Vostok ice core for the past 160,000 years (adopted from De Angelis et al. 1987). Measured Al concentrations were converted to Fe concentrations according to the average continental crust composition. The negative correlation of CO_2 and Fe supports the 'iron hypothesis' (see text).

uptake by the oceans. A comparison of iron and CO_2 concentrations of the past 160,000 years recorded within an Antarctic ice core revealed a strikingly negative correlation (Fig. 7.7) which supports the 'iron hypothesis'.

So far, dissolved iron has been discussed with respect to the assimilation by phytoplankton. The chemical state of bioavailable dissolved species is presently a matter of intensive studies and discussions. Due to thermodynamic reasons concentrations of free ions of dissolved iron are extremely low under oxic and pH-neutral conditions. A discussion paper by Johnson et al. (1997) reviews regional distributions and depth profiles of dissolved iron and points out that at greater depth the iron concentrations always remain constant of ~ 0.6 nM. Other elements with such short residence time (100 to 200 years) typically continuously decrease with depth and age. This suggests a substantial decrease in the iron removal rate below this concentration. As organic ligands with a binding capacity of 0.6 nM Fe have been found (Rue and Bruland 1995; Wu and Luther 1995), iron-organic complexes are regarded to be of great importance for the distribution of dissolved iron. Additional evidence for the interaction with dissolved organic molecules comes from the study of iron uptake mechanisms by organisms. To make dissolved iron more accessible, microorganisms have acquired the ability to synthesize chelators which complex ferric iron of solid phase. These chelators are commonly called siderophores and consist of a low-molecular-mass compound with a high affinity for ferric iron. Siderophores are secreted out of the microorganism where they form a complex with ferric iron. After transport into the cell, the chelated ferric iron is enzymatically reduced and released from the siderophore, which is secreted again for further complexation. For the open ocean environment ferric iron availability by the secretion of siderophores was shown for phytoplankton (Trick et al. 1983), as well as for bacteria (Trick 1989). Kuma et al. (1994) showed that total natural organic Fe^{3+}-chelators are abundant in open ocean regions of the eastern Indian Ocean and the western North Pacific Ocean where they control the dissolved iron concentration. Recent experiments have explored the mechanisms of the dissolution of iron oxyhydroxides under variable light and chelator conditions and it was concluded that the interplay of siderophores and light controls the overall process (Borer et al. 2005).

7.4 The Early Diagenesis of Iron in Sediments

The fundamental work by Froelich et al. (1979) established a conceptual model for the organic matter respiration in marine sediments which has been modified, verified and extended in numerous aspects since then. Froelich and colleagues found a succession of electron acceptors used by dissimilatory bacteria according to their energy gain. Consequently, a biogeochemical zonation of the sediment results where O_2, NO_3^-, bioavailable Mn(IV) and Fe(III) and SO_4^{2-} diminish successively with depth. Apart from the consumption of electron acceptors the production of reduced species such as NH_4^+, Mn^{2+}, Fe^{2+}, HS^- and CH_4 occurs. These components may be reoxidized abiotically under given thermodynamic conditions. As will be shown, these reoxidation reactions can also be microbiologically catalyzed. It is important to note that for the investigation of iron reactivity a differentiation of biotic and abiotic reactions is inherently important but often very difficult to achieve. Another considerable question with respect to the iron reactivity in sediments concerns the bioavailable fraction of iron bearing minerals. So far, it could be shown that ferric iron of iron oxides as well as certain sheet silicates can be used by dissimilatory iron reducing bacteria but their quantities and rates of reduction vary significantly. A final discussion of this section will compare different depositional environments with respect to the importance of dissimilatory iron reduction, chemical reduction and the availability of ferric iron.

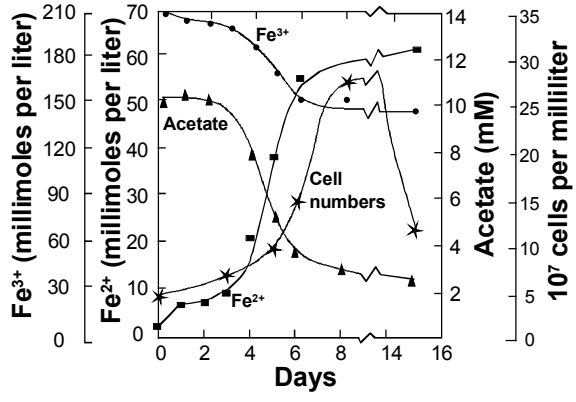

Fig. 7.8 Iron reduction by GS-15 with acetate as electron donor (adopted from Lovley and Philips 1988).

7.4.1 Dissimilatory Iron Reduction

Iron (and manganese) can be reduced enzymatically by various pathways, which are summarized in great detail by Lovley (1991). One of the prerequisites is the direct contact between the bacteria and solid phase ferric iron (Munch and Ottow 1982). The following given equations shall be considered as representative for a series of reactions within each group.

1. Fermentative Fe^{3+}-reduction:

$$C_6H_{12}O_6 + 24Fe^{3+} + 12H_2O \Rightarrow 6HCO_3^- + 24Fe^{2+} + 30H^+ \quad (7.1)$$

2. Sulfur-oxidizing Fe^{3+}-reduction:

$$S^0 + 6Fe^{3+} + 4H_2O \Rightarrow HSO_4^- + 6Fe^{2+} + 7H^+ \quad (7.2)$$

3. Hydrogen-oxidizing Fe^{3+}-reduction:

$$H_2 + 2Fe^{3+} \Rightarrow 2H^+ + 2Fe^{2+} \quad (7.3)$$

4. Organic-acid-oxidizing Fe^{3+}-reduction:

$$acetate^- + 8Fe^{3+} + 4H_2O \Rightarrow 2HCO_3^- + 8Fe^{2+} + 9H^+ \quad (7.4)$$

5. Aromatic-compound-oxidizing Fe^{3+}-reduction:

$$phenol + 28Fe^{3+} + 17H_2O \Rightarrow 6HCO_3^- + 28Fe^{2+} + 34H^+ \quad (7.5)$$

For the case of fermentative Fe(III)-reduction it is important to note that during fermentation Fe(III) only serves as a minor sink for electrons and that organic substrates are primarily transformed to organic acids or alcohols.

A review of organisms reducing Fe(III), the respective electron donors and the applied forms of Fe(III) is given by Lovley (1987) and Lovley et al. (1997). In Figure 7.8 a typical result of ferric iron reduction mediated by a distinct ferric iron reducing bacteria (i.e. *Geobacter metallireducens*) and an appropriate electron donor (i.e. acetate) is shown. Note that the reproduction (cell numbers) ceases although acetate and ferric iron are still present. This is a general observation, which is explained by the limited bioavailability of the ferric iron fraction (section 7.4.2.2). Figure 7.9 represents a model for the degradation of natural organic matter with ferric iron as sole electron acceptor (Lovley 1991). The primary organic matter is hydrolyzed to smaller compounds such as sugars, amino and fatty acids, and aromatic

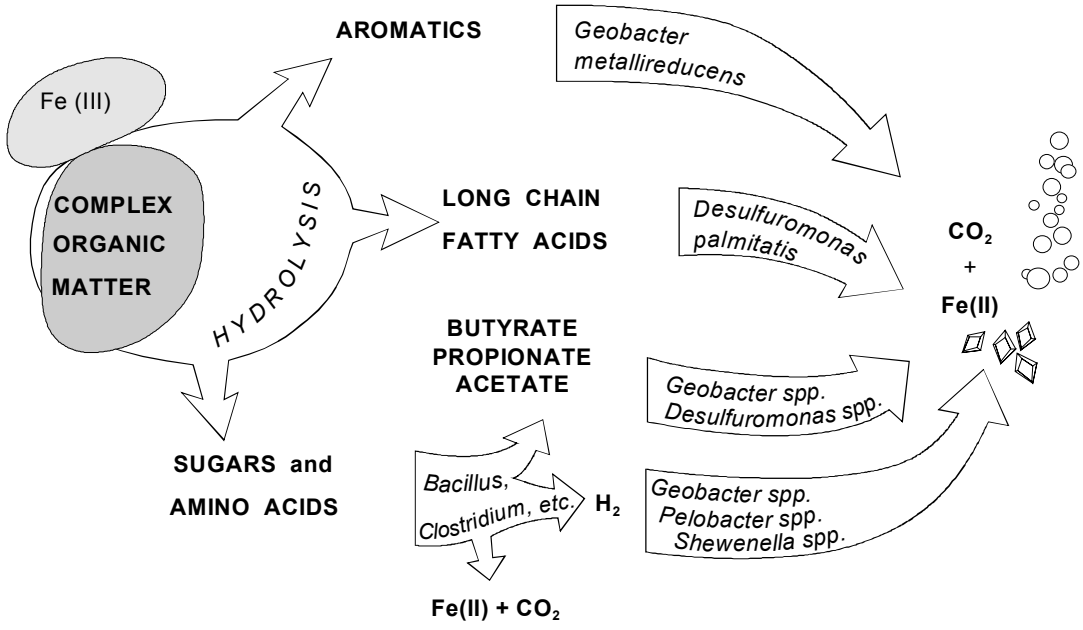

Fig. 7.9 Schematic model for the oxidation of complex organic matter with ferric iron as sole electron acceptor (adopted from Lovley 1997).

compounds through the activity of hydrolytic enzymes which are produced by a variety of microorganisms. Subsequently, these intermediate products can be used for the dissimilatory ferric iron reduction.

7.4.2 Solid Phase Ferric Iron and its Bioavailability

Solid phase ferric iron is present in various iron bearing minerals and amorphous phases of marine sediments. Two major groups can be distinguished: Iron oxyhydroxides (including iron oxides) and (sheet) silicates. As the iron bearing mineral assemblage varies considerably among different depositional environments the microbiological availability of specific Fe(III)-bearing compounds can be highly variable.

7.4.2.1 Properties of Iron Oxides

During terrestrial weathering a minor amount of the released iron from silicates (biotite, pyroxene, amphibole, olivine) is incorporated into clay minerals and a major fraction serves for the formation of iron oxides. Among iron oxides goethite (α-FeOOH) and hematite (α-Fe_2O_3) are the most abundant and are mostly associated with each other. Lepidocrocite (γ-FeOOH), maghemite (γ-Fe_2O_3) and magnetite ($Fe^{2+}Fe_2^{3+}O_4$) are generally quantitatively less abundant. Yet, with respect to the magnetization of the sediment magnetite and maghemite are of great importance

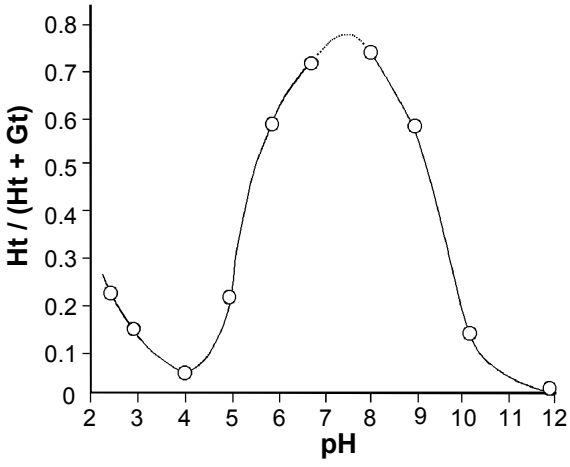

Fig. 7.10 Recrystallization products of a ferrihydrite suspension after 441 days. Aging causes a formation of hematite (Ht) and goethite (Gt) depending on the pH of ambient water (adopted from Schwertmann and Murad 1983).

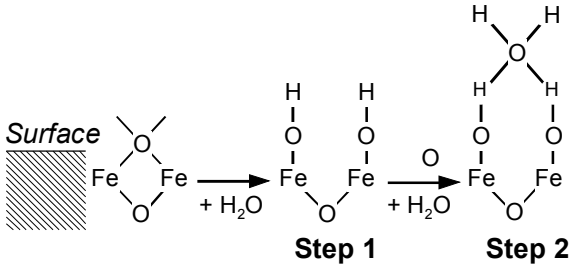

Fig. 7.11 In the presence of water the iron oxide surface is hydroxylated (step 1) and subsequently H_2O is adsorbed (step 2) (redrawn from Schwertmann and Taylor 1989).

due to their ferrimagnetic character (chapter 2). Iron phases precipitating from solution are collectively called iron oxyhydroxide. By means of mineralogical identification methods (X-ray diffraction, infrared and Mössbauer spectroscopy) the precipitate may be completely amorphous representing a ferric gel or it may be a poorly crystallized, water containing phase such as ferrihydrite ($5Fe_2O_3 \cdot 9H_2O$). Formerly this fraction was called 'amorphous Fe(III)hydroxide' (Böhm 1925). Aging causes these earliest precipitates to increase their crystallinity, which means an increase in the ordering of the crystal lattice. Depending on the pH-value of ambient water the resulting proportion of goethite versus hematite varies. Hematite is favored under seawater conditions (Schwertmann and Murad 1983; Fig. 7.10). The effect of aging also explains the observation of a decrease in the highly reactive Fe-oxide fraction with water depth and distance to the coast although the total fraction of Fe-oxides and total iron concentration increases (Haese et al. 2000). With respect to the adsorption of anions and cations as well as to organic ligand formation (see below) it is important to know an approximate dimension of the specific surface area of iron oxides / oxyhydroxide. Crosby et al. (1983) determined specific surface areas for iron oxyhydroxide synthesized under natural conditions revealing 159-234 m^2g^{-1} for precipitates from Fe^{3+} solutions and 97-120 m^2g^{-1} for precipitates from Fe^{2+} solutions. Natural samples showed a range from 6.4-164 m^2g^{-1}.

Physical, chemical and mineralogical properties of the iron oxides can be variable. Aluminium (Al(III)) may substitute isomorphically for Fe(III) due to very similar ionic radii (Fe(III): 0.73 Å; Al(III): 0.61 Å) and the same valence. Norrish and

Taylor (1961) found a maximum of one-third mole percent Al substitution for Fe within goethite and a maximum of one-sixth substitution was determined for hematite in soils (Schwertmann et al. 1979). As a product of terrestrial weathering magnetites usually contain minor amounts of Ti(IV) (ionic radius: 0.69 Å) as a substitution for Fe which is then called titano-magnetite. In contrast, bio-mineralized magnetite is a pure iron oxide. Different colors of iron oxides / oxyhydroxide are immediately apparent in nature. This holds true for different pure iron oxides, for different grain sizes of one oxide (e.g. goethite) as well as for distinct substitutions for Fe, e.g. by Mn or Cr (Schwertmann and Cornell 1991). The color of synthetic minerals and natural sediment can be quantitatively determined by reflectance spectroscopy (e.g. Morris et al. 1985).

In the presence of water the surface of an iron oxide is completely hydroxylated which can be understood as a two-step reaction which is shown schematically in Fig. 7.11.

As iron oxides / oxyhydroxide have a very high affinity for the adsorption of anions as well as cations under natural conditions the early diagenetic reactivity of iron is often of great significance for the behavior of compounds such as trace metals, phosphate and organic acids. The adsorption on iron oxides is caused by the hydroxylation of the mineral surface (S-OH). Depending on the pH of ambient water protonation or deprotonation occurs according to

$$\text{S-OH} + \text{H}^+ \quad \Leftrightarrow \quad \text{S-OH}_2^+ \qquad (7.6)$$

$$\text{S-OH} + \text{OH}^- \quad \Leftrightarrow \quad \text{S-O}^- + \text{H}_2\text{O} \qquad (7.7)$$

As a result, the surface charge and the surface potential vary depending on the concentration of H^+ ions in solution. Apart from the pH the surface charge is influenced by the concentration of the electrolyte and the valence of ions in solution. pH-values where the net surface charge is zero are called points of zero charge (pzc). For pure synthetic iron oxides these vary between a pH of 7 and 9. An excess of positive or negative charge is balanced by the equivalent amount of anions or cations. As representative for the adsorption of cations (Cu^{2+}), anions ($H_2PO_4^-$) and organic compounds (oxalate) the following reactions are given:

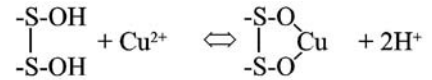

(7.8)

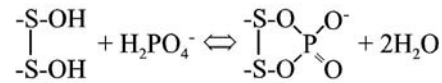

(7.9)

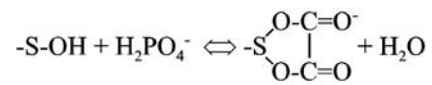

(7.10)

As the complexation of cations causes a release of H^+ and anions compete with surface bound hydroxyl groups ('ligand exchange') the adsorption is strongly pH-dependant (see above). As a result, anions are preferably adsorbed at lower pH-values whereas cations are primarily adsorbed at higher pH values (Fig. 7.12).

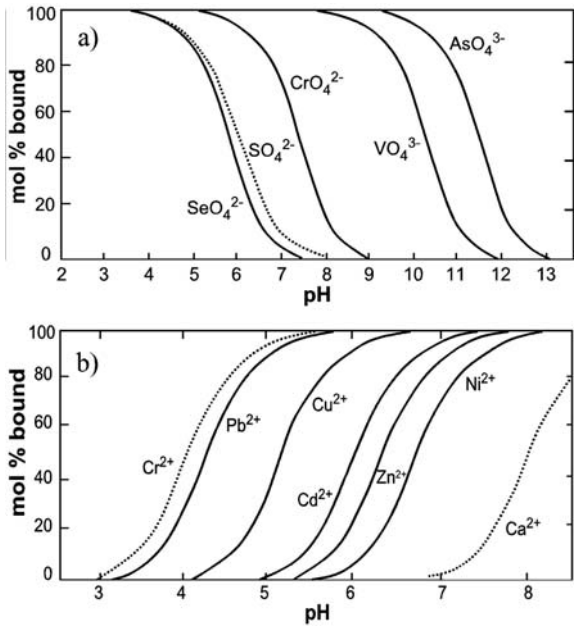

Fig. 7.12 The pH dependence of anion (a) and cation (b) sorption on hydrous ferric oxide (adopted from Stumm and Morgan 1996).

7.4.2.2 Bioavailability of Iron Oxides

As dissimilation is a biological process used to gain electrons for cell energetic functions, the energy gain from the induced reactions is noteworthy. The following reactions and their respective standard free energy, ΔG^o, values are given to provide an overview of the energy gain due to the reaction with various iron oxyhydroxide / oxides.

$$4\text{Fe(OH)}_3 + \text{CH}_2\text{O} + 7\text{H}^+ \Rightarrow 4\text{Fe}^{2+} + \text{HCO}_3^- + 10\text{H}_2\text{O} \qquad (7.11)$$

ΔG^0: (-376) - (-228) kJ mol^{-1}

$$4FeOOH + CH_2O + 7H^+ \Rightarrow 4Fe^{2+} + HCO_3^- + 6H_2O \quad (7.12)$$

ΔG^0: (-387) - (-239) kJ mol^{-1}

$$2\alpha\text{-}Fe_2O_3 + CH_2O + 7H^+ \Rightarrow 4Fe^{2+} + HCO_3^- + 4H_2O \quad (7.13)$$

ΔG^0: -236 kJ mol^{-1}

$$2Fe_3O_4 + CH_2O + 11H^+ \Rightarrow 6Fe^{2+} + HCO_3^- + 6H_2O \quad (7.14)$$

ΔG^0: -328 kJ mol^{-1}

ΔG^0 values were adopted from Stumm and Morgan (1996). For $Fe(OH)_3$ and FeOOH a range of free energy is given as the solubility products $K_s = [Fe^{3+}]\ [OH^-]^3$ range from $10^{-37.3}$ to $10^{-43.7}$ depending on the mode of preparation, age and molar surface. For example, aged goethite (α-FeOOH) reveals a ΔG^0_f of -489 kJ mol^{-1} whereas for freshly precipitated amorphous FeOOH a value of -462 kJ mol^{-1} was determined (Stumm and Morgan 1996). The variability of FeOOH thermodynamic properties is a result of the metastability of freshly precipitated ferric iron phases (chapter 7.4.2.1, Fig. 7.10).

By means of microbial cultures growing on the various iron oxides as terminal electron acceptors it has been shown that they all can be used for the purpose of dissimilation (e.g. Lovley 1991; Kostka and Nealson 1995). Yet, it was generally found that the ferric iron phases were reduced at different rates and to varying degrees. Consequently, Ottow (1969) determined the following sequence of biological availability: $FePO_4{\cdot}4H_2O$ > $Fe(OH)_3$ > lepidocrocite (γ-FeOOH) > goethite (α-FeOOH) > hematite (Fe_2O_3). Note that the Fe-P phase may sequester significant amounts of P out of the nutrient loaded freshwater part of an estuary, but under brackish and marine conditions this phase is not stable as it rapidly transforms under the influence of free sulfide (Hyacinthe and Van Cappellen, 2004). Within natural soil samples a preferential reduction of amorphous to crystalline iron oxides was found (Munch and Ottow 1980). Later, Roden and Zachara (1996) discovered the importance of the solid phase specific surface area for the degree of reducibility. The greater the specific surface area was the more reduced ferric iron was determined (Fig. 7.13). Additionally, they could show that after rinsing the solid phase, which could not be reduced any further, dissimilatory reduction of the original ferric iron was continued. They concluded that the reduction of iron oxides is limited by the adsorption of some components, possibly Fe^{2+}, which inhibits further microbial access. This finding also explains the results of Munch and Ottow (1980, see above) because amorphous and poorly crystalline phases are usually characterized by a higher specific surface area than well crystallized phases, and the greater the specific surface area the more can be adsorbed. This early finding agrees with the results of a recent study, which identified nanophase goethite with diameters < 12 nm to be the predominant authigenic iron oxyhydroxide in freshwater and marine environments (van der Zee et al. 2003).

Once a framework for the availability of iron oxides is established, the kinetics of individual reactions provides insight into reaction rates and rate limiting steps for the overall reactivity of iron. Here, the kinetics of microbial iron oxide reduction is explored and in section 7.4.4.1 analog information are provided for the reduction by sulfide and ligands. Building on previous experimental results demonstrating the control of mineral surface area for the degree of iron reduction (Roden and Zachara 1996; Fig. 7.13), it was shown, that also the rate of microbial iron reduction in natural sediments is of first-order and controlled by the mineral surface area (Roden and Wetzel

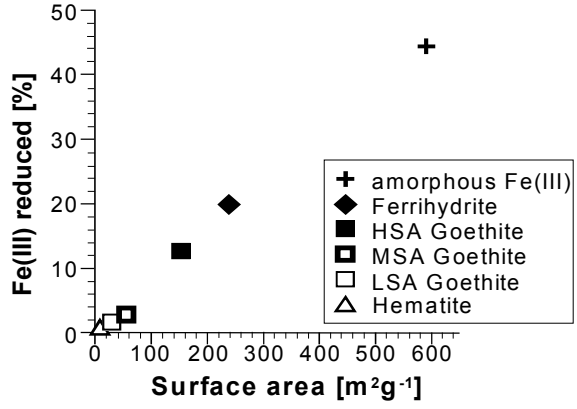

Fig. 7.13 The dependence of solid phase ferric iron reducibility from the specific surface area of iron oxyhydroxide / oxides (redrawn from Roden and Zachara 1996). HSA, MSA, and LSA represent high, medium, and low specific surface area.

2002). Kinetic experiments with synthetic iron oxyhydroxides have shown that the initial microbial reduction rate increases with increasing initial ferric iron concentration up to a given maximum reduction rate (Bonneville et al. 2004). This observation was explained by a saturation of active membrane sites with Fe(III) centers. The respective reaction was best described with a Michaelis-Menten rate expression with the maximum reduction rate per cell positively correlating with the solubility of the iron oxyhydroxides (Bonneville et al. 2004). Kinetic studies involving iron are not only inherently important to describe reaction pathways and to derive rate constants, which can be used in models. Kinetic studies also increasingly focus on iron isotopic fractionation to better understand the iron isotopic composition of ancient sediments, which may assist in the reconstruction of paleo-environments. Importantly, iron isotope fractionation occurs in abiotic and biotic processes; the degree of isotopic fractionation depends on individual reaction rates and the environmental conditions, e.g. whether reactions take place within an open or closed system (Johnson et al. 2004).

7.4.2.3 The Bioavailability of Sheet Silicate Bound Ferric Iron

As early as in 1972 Roth and Tullock published results on the chemical reduction of smectites. Subsequently, Rozenson and Heller-Kallai (1976a,b) studied the potential of reduction and reoxidation in various dioctahedral smectites with the aid of different reducing and oxidizing agents. Concurrent with the change of the intercrystalline redox state a change of the smectite color was observed. Oxidized smectites showed a white or yellowish color whereas the reduced smectites revealed a greenish-grey or black color. To balance the intercrystalline charge (de-) protonation was postulated. Additionally, as a consequence of smectite reduction a decrease of the specific surface area and the swellability in water, as well as an increase of nonexchangeable Na^+ was found (Lear and Stucki 1989). A potential importance of smectite redox reactivity in natural sediments was first pointed out by Lyle (1983) for sediments of the eastern equatorial Pacific where a distinctive color transition from tan (above) green-gray (below) was found in near-surface sediments. König et al. (1997) conducted a high resolution Mössbauer-spectroscopy study for one core from the Peru Basin which revealed a present-day reduction of 42 % of total iron which can be differentiated into an immobile fraction (36 %) consisting of smectite bound iron and a mobile fraction (16 %) which diffuses back into the oxidized upper sediment layer. Evidence for the bioavailability of ferric iron bound to smectites was given by Kostka et al. (1996). During culturing of an iron reducing bacteria (*Shewanella putrefaciens* strain MR-1) on smectite as a sole electron acceptor a reduction of Fe^{3+} by 15 % within the first 4 hours and a total of 33 % after two weeks occurred.

7.4.3 Iron Reactivity towards S, O_2, Mn, NO_3^-, P, HCO_3^-, and Si-Al

The (microbial) dissimilatory iron reduction was shown in the previous section. In this section the reactions with major oxidants and reductants will be introduced. Additionally, the interactions between iron and phosphorus, as well as the formation of siderite and iron-bearing sheet silicates will be pointed out briefly to show to the variety of reactions in marine sediments coupled the reactivity of iron.

7.4.3.1 Iron Reduction by HS^- and Ligands

Apart from the dissimilatory iron reduction (section 7.4.1) iron oxides can be dissolved by protons, ligands and reductants. Dissolution reactions by protons and ligands are generally considered to be the rate-determining step for weathering processes. For iron bearing minerals in marine sediments proton-promoted dissolution is of no importance due to prevailing neutral or slightly alkaline conditions. Ligands (e.g. oxalates and citric acid) are by-products of biological decomposition and dissolve iron oxides by primary surface complexation onto the iron oxide surface resulting in a weakening of the Fe-O bond which is followed by a detachment of Fe^{3+}-ligand. Reductive dissolution (e.g. by HS^-, ascorbate, and dithionite) is characterized by primary surface complexation followed by an electron transfer from the reductant to ferric iron and detachment of Fe^{2+}. The three pathways of Fe(III) (hydr)oxide dissolution are shown in Fig. 7.14.

Experimental determination of reduction rates (e.g. Pyzik and Sommer 1981; Dos Santos Afonso and Stumm 1992; Peiffer et al. 1992) reveal rates under well defined conditions and information on the reaction kinetics. Under natural conditions the

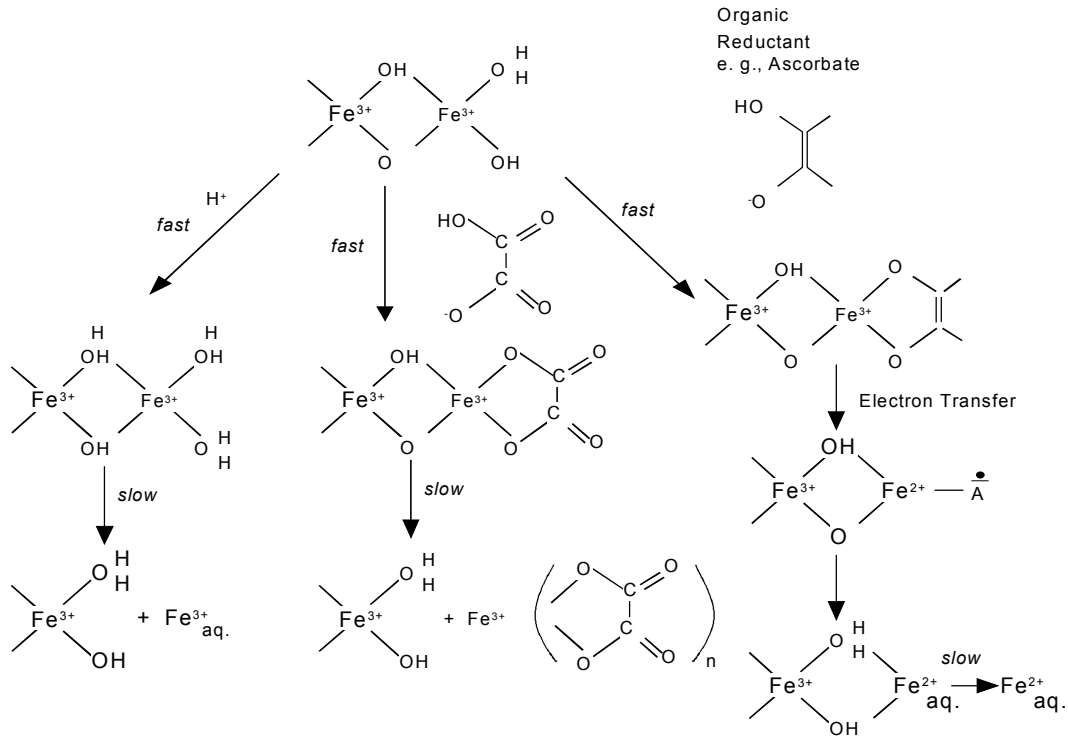

Fig. 7.14 Pathways of Fe(III)(hydr)oxide dissolution. From the left to right: Proton-, ligand- (here: oxalate), and reductant- (here: ascorbate) promoted dissolution is initiated by surface complexation. The subsequent step of detachment ($Fe^{3+}_{aq.}$, Fe^{3+}-ligand, $Fe^{2+}_{aq.}$) is rate determining. Note that the shown pathways of dissolution are fundamental for the described extractions (chapter 7.5) (adopted from Stumm and Morgan, 1996).

composition of dissolved compounds in solution is complex and may have significant influence on the dissolution rate. Biber et al. (1994) demonstrated the inhibition of reductive dissolution by H_2S and the ligand-promoted dissolution by EDTA due to the presence of oxoanions (e.g. phosphate, borate, arsenate) (Fig. 7.15 a,b).

A sequence of iron mineral reactivity towards sulfide was proposed more than 10 years ago (Canfield et al. 1992), which was later extended (Raiswell and Canfield 1996), and recently revised (Poulton et al. 2004). The revised sequence particularly accounts for the mineral surface area and can be grouped into two fractions excluding

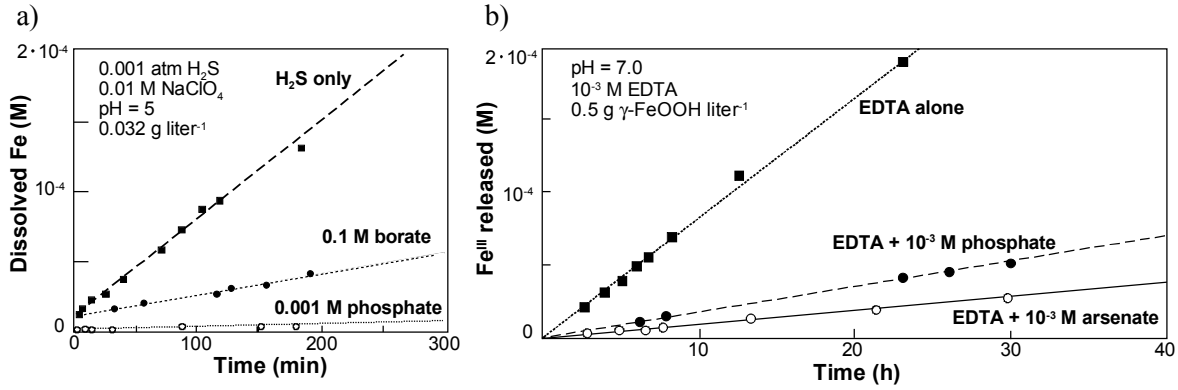

Fig. 7.15 Inhibitation of reductive- and ligand-promoted dissolution of iron oxides by oxoanions. a: The dissolution of goethite by H_2S is inhibited by borate and phosphate. b: The dissolution of lepidocrocite by EDTA is inhibited by phosphate and arsenate (adopted from Stumm and Morgan 1996, original data from Biber et al., 1994).

Table 7.1 Reactivity of iron minerals towards sulfide (1000 ìM $ÓH_2S$, pH 7.5, 25°C) according to 1: Poulton et al. (2004), 2: Canfield et al. (1992), and 3: Raiswell and Canfield (1996). The 'poorly-reactive silicate fraction' was determined operationally as $(Fe_{HCl,\ boiling} - Fe_{Dithionite}) / Fe_{total}$

Iron Mineral / fraction	Half life, $t_{1/2}$
Hydrous Ferric Oxide[1]	5.0 minutes
2-line Ferrihydrite[1]	12.3 hours
Lepidocrocite[1]	10.9 hours
Goethite[1]	63 days
Magnetite [1]	72 days
Hematite [1]	182 years
Sheet silicates[2]	10 000 years
poorly-reactive silicate fraction[3]	2.4 x 10^6 years

iron bearing silicates: The poorly crystalline hydrous ferric oxide, 2-line ferrihydrite and lepidocrocite are reactive on a time scale of minutes to hours, whereas goethite, hematite and magnetite are reactive on a time scale of tens of days. In Table 7.1 the reactivity of iron oxyhydroxides and iron bearing silicate minerals towards sulfide is expressed as half-life ($t_{1/2}$).

The presence of iron minerals and their respective reactivity towards sulfide is of greatest importance for the pore water chemistry and the limitation for pyrite formation. In case of reactive iron rich sediments dissolved iron may build-up in pore water and dissolved sulfide is hardly present although sulfate reduction occurs. In contrast, in sediments characterized by a low content of reactive iron dissolved sulfide can build-up instead of dissolved iron (Canfield 1989). The degree of pyritisation (DOP) was originally defined by Berner (1970) and was later modified by Leventhal and Taylor (1990) and Raiswell et al. (1994). DOP is now defined as:

$$DOP = \frac{Fe_{pyrite}}{Fe_{pyrite} + Fe_{dithionite-soluble}} \qquad (7.15)$$

A DOP-value of 1 means a complete pyritisation of reactive iron, which has been found in sediments overlain by anoxic-sulfidic bottom water (Raiswell et al., 1988). In sediments exposed to sulfide for more than one million years silicate-bound iron has only been partially turned into pyrite (Raiswell and Canfield 1996). This observation is explained by an overall slow rate of pyritisation of silicate-bound iron, which is influenced by the mineral assemblage, degree of crystallinity and grain size. This clearly states the range of silicate iron reactivity towards sulfide, which is influenced by the mineral assemblage, degree of crystallinity and grain size.

7.4.3.2 Iron Oxidation by O_2, NO_3^-, and Mn^{4+}

The reaction of dissolved Fe^{2+} with oxygen is known to be fast and its rate was determined in sea-water by Millero et al. (1987):

$$\frac{-d[FeII]}{dt} = \frac{K_H[O_{2\,aq.}]}{[H^+]^2} \cdot [FeII] \qquad (7.16)$$

at 20 °C, k_H=3x10^{-12} mol $min^{-1}liter^{-1}$. At a temperature of 5 °C the rate decreases by about a factor of 10. As the oxidation rate (-d[FeII]/dt) is inversely proportional to the power of the proton concentration ($[H^+]^2$) the importance of the pH becomes obvious. The lower the pH (= - log $[H^+]$), the lower is the rate of ferrous iron oxidation. Therefore, within a ferrous iron solution with a very low pH-value, e.g. acidified with HCl, the reaction is so slow that oxidation under air atmosphere is negligible over weeks. Under pH neutral conditions this reaction is so fast that dissolved iron may only escape from the sediment into the bottom water if the oxygen penetration depth is very little or even anoxic bottom water conditions are given. The effects on iron, manganese, phosphate and cobalt fluxes during a controlled decrease of oxygen bottom water concentration and the importance of the diffusive boundary layer within a benthic flux-chamber (see chapter 3) were studied by Sundby et al. (1986). They could demonstrate that due to a decrease of diffusive oxygen flux into the sediment manganese release increased prior to iron according to thermodynamic predictions (Balzer 1982). Stirring within a flux-chamber controls the thickness of the benthic boundary layer and thus the diffusive flux of oxygen into the sediment. A decrease or even an interruption of stirring results in a significant increase of benthic efflux of redox-sensitive constituents such as iron and manganese.

Buresh and Moraghan (1976) showed the thermodynamic potential of ferrous iron oxidation by nitrate, yet the reaction is not spontaneous. In the presence of solid phase Cu(II), Ag(I), Cd(II) , Ni(II), and Hg(II) serving as catalysts ferrous iron can reduce nitrate rapidly (Ottley et al. 1997). Similarly, the formation of a Fe(II)-lepidocrocite (γ-FeOOH)

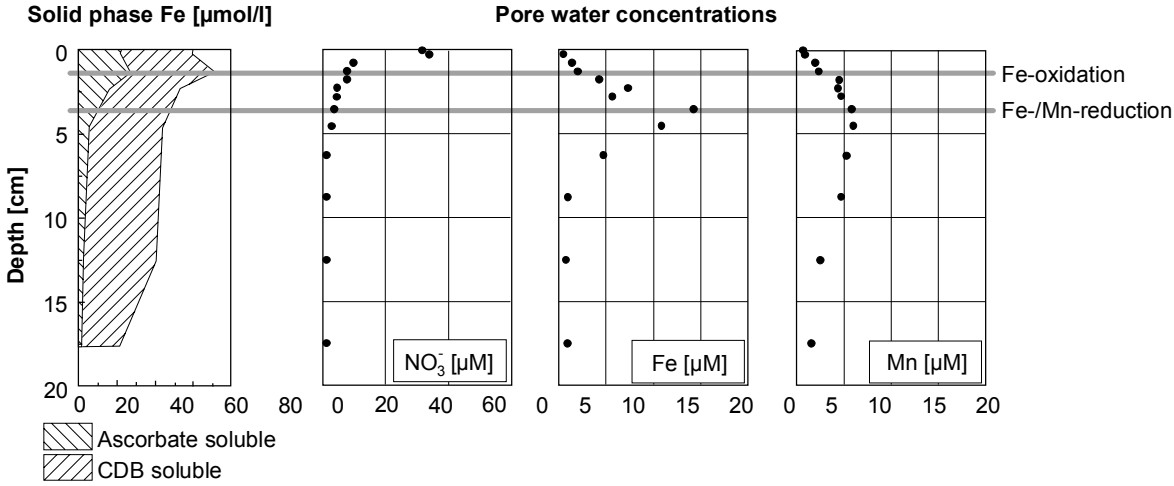

Fig. 7.16 Pore water and extraction results from hemipelagic sediments off Uruguay (redrawn from Haese et al. 2000). Dissolution and precipitation of Fe is reflected by the easy reducible iron oxyhydroxide fraction whereas less reducible iron oxides soluble by subsequent citrate/dithionite/bicarbonate (CDB) extraction remain constant. A concurrent liberation of Mn and Fe indicates dissimilatory iron reduction and subsequent iron reoxidation by manganese oxides, which results in the build-up of Mn^{2+}. Under these conditions the actual dissimilatory iron reduction rate is higher than deduced from iron pore water gradients.

surface complex was found to catalyze chemodenitrification (Sørensen and Thorling 1991). The potential significance of microorganisms inducing ferrous iron oxidation was pointed out within the last years (Widdel et al. 1993; Straub et al. 1996). Ferrous iron was found to serve as electron donor in cultures of nitrate-reducing bacteria. Even in the presence of acetate as typical electron donor ferrous iron was additionally oxidized. This implies

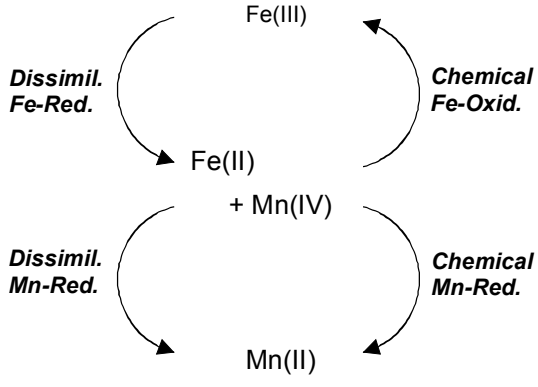

Fig. 7.17 Interaction of dissimilatory Fe / Mn reduction and abiotic reaction of Fe^{2+} with Mn(IV). Note that additional interactions with species and microbial processes typically occuring in surface sediments (e.g. sulfate reduction and subsequent reactions of HS^-) are not considered and that Mn(IV) is not replenished.

that iron oxide formation typically occurring at the interface of nitrate and iron bearing pore water is at least in parts microbially mediated. Ehrenreich and Widdel (1994) have described a microbial mechanism of pure anaerobic oxidation by iron oxidizing photoautotrophs. This exciting observation challenges the conviction that the earliest iron oxidation on earth occurred during the build-up of free oxygen. One may now speculate that the accumulation of the Banded Iron Formation (Archaic age, ~ 3 billions years B.P.) was microbiologically induced under suboxic/anoxic conditions. Similarly, manganese oxidation rates in natural environments were determined to be considerably higher than determined in laboratory studies under abiotic conditions implying a microbially mediated manganese oxidation (Thamdrup et al. 1994; Wehrli et al. 1995).

Ferrous iron oxidation by manganese oxide was found to be especially fast as long as no iron oxyhydroxide precipitates, which presumably blocks reactive sites on the manganese oxide surface (Postma 1985). The oxidation of ferrous iron by manganese oxide has been proven to be important for the interpretation of pore water profiles and the precipitation of authigenic phases (Canfield et al. 1993a; Haese et al. 2000; van der Zee 2005). In Fig. 7.16 pore water profiles of iron and manganese reveal concurrent liberation of the

two elements which was attributed to dissimilatory iron reduction and subsequent iron reoxidation by manganese oxides which in turn results in the production of $Mn^{2+}_{aq.}$.

Similar to the possibility of concurrent reduction of sulfate and ferric iron by a culture of a single bacteria (Coleman et al. 1993; see section 7.4.3.4) other iron reducing bacteria were found to additionally maintain dissimilation with more than one electron acceptors under suboxic conditions (Lovley and Phillips 1988) or even under oxic conditions (Myers and Nealson 1988a). In the presence of Fe(III) and Mn(IV) strain MR-1 was found to reduce both but additional manganese reduction occurred due to the immediate abiotic reaction with released Fe^{2+} (Myers and Nealson 1988b). The interactions of biotic and abiotic reactions are shown in Fig. 7.17.

7.4.3.3 Iron-bound Phosphorus

In section 7.4.2.1 the theoretical significance of phosphate adsorption onto iron oxides was illustrated. Numerous studies on natural sediments suggest that iron oxides control phosphate pore water and solid phase concentrations, as well as the overall sedimentary phosphate cycle (Krom and Berner 1980; Froelich et al. 1982; Sundby et al. 1992; Jensen et al. 1995; Slomp et al. 1996a,b). A generalized representation of the sedimentary phosphorus cycle is shown in Fig. 6.11. Apart from the Fe-bound P, organic P and authigenic carbonate fluorapatite are the principal carriers of solid phase P. HPO_4^{2-} is the predominant dissolved P species under sea water conditions (Kester and Pytkowicz 1967).

The following information and simple calculation allows the reader to assess and understand the important role of iron oxyhydroxides and their interactions with phosphorous: A maximum of 2.5 - 2.8 µmol m^{-2} of adsorbed phosphate on iron oxides were found (Goldberg and Sposito 1984; Pena and Torrent 1984). In order to approximate a maximum adsorbed phosphate concentration in the sediment one can assume 1 cm^3 of sediment with a porosity of 75 %, a dry weight density of 2.65 g cm^{-3}, 50 $\mu mol/g_{Sediment}$ Fe bound to iron oxides and an iron oxide specific surface area of 120 m^2 g^{-1} (see section 7.4.2.1). For the wet sediment we can calculate an iron concentration of 33 µmol cm^{-3} which is bound to iron oxides. This fraction has a specific surface area of ~ 0.22 m^2 within 1 cm^3 of wet sediment which may then adsorb up to ~ 0.57 µmol P (assuming an adsorption capacity of 2.6 µmol P per square meter of iron oxide). For a comparison of adsorbed and dissolved phosphate concentration we can furthermore assume a concentration of 5 µM phosphate within the interstitial water which is equivalent to 0.0037 µmol cm^{-3} of wet sediment. Consequently, the adsorbed fraction of phosphate can be more than two orders of magnitude greater than the dissolved fraction due to the presence of iron oxides. In reality, the ratio of Fe bound to poorly crystalline iron oxides and P bound by these phases has been determined to be ~ 10Fe : 1P for coastal and shelf sediments (Slomp et al., 1996a). This differs significantly from the given theoretical sample in which we find a ratio of 58 (33 µmol Fe : 0.57 µmol P per 1 cm^3). Either P is additionally bound in the crystalline lattice of the iron oxides (i.e. Torrent et al., 1992) or the adsorption capacity for P in shelf sediments is much greater than derived from the calculated example. In the latter case, one must conclude that the specific surface area of Fe oxides is higher than assumed as another quantitatively important adsorbent of P in sediments is not likely. Instead of 120 m^2 g^{-1} iron oxide one needs to encounter a specific surface area of 650-700 m^2 g^{-1} to justify such high P adsorption.

7.4.3.4 The Formation of Siderite

In the marine environment siderite ($FeCO_3$) is hardly found relative to iron sulfides because it is thermodynamically not stable in the presence of even low dissolved sulfide activities. Postma (1982) proved the calculation of the solubility equilibrium between siderite and ambient pore water chemistry to be a reliable approach for the investigation of present-day siderite formation. In salt marsh sediments where the influence of salt and fresh water varies temporarily and spatially the formation of siderite and pyrite are closely interlinked. Mortimer and Coleman (1997) demonstrated that siderite precipitation is microbiologically induced. They could show that $\delta^{18}O$ values of siderite precipitated during the culturing of one specific iron-reducing microorganism, *Geobacter metallireducens*, were distinctively lower than expected according to equilibrium fractionation between siderite and water (Carothers et al. 1988) which is a contradiction to a pure thermodynamically induced reaction.

In fully marine systems siderite formation is probable to occur below the sulfate reduction zone where dissolved sulfide is absent, if reactive iron is still present and the Fe/Ca-ratio of pore water is high enough to stabilize siderite over calcite (Berner 1971). The coexistence of siderite and pyrite in anoxic marine sediments was shown by Ellwood et al. (1988) and Haese et al. (1997). Both studies attribute this observation to the presence of microenvironments resulting in different characteristic early diagenetic reactions next to each other within the same sediment depth. It appears that in one microenvironment sulfate reduction and the formation of pyrite is predominant, whereas at another site dissimilatory iron reduction and local supersaturation with respect to siderite occurs. Similarly, the importance of microenvironments has been pointed out for various other processes (Jørgensen 1977; Bell et al. 1987; Canfield 1989; Gingele 1992).

Apart from microenvironments, an explanation for the concurrent dissimilatory sulfate and iron reduction was provided by Postma and Jakobsen (1996). They demonstrated that the stabilities of iron oxides are decisive with respect to iron and/or sulfate reduction assuming that the fermentative step and not the overall energy yield is overall rate limiting. Additionally, it shall be noted that the typical sulfate reducing bacteria *Desulfovibrio desulfuricans* was found to reduce iron oxide enzymatically contemporarily or optionally (Coleman et al. 1993). When only very small concentrations of H_2 as sole electron donor were available iron oxide instead of sulfate was used as electron acceptor by *D. desulfuricans*.

7.4.3.5 The Formation of Iron Bearing Aluminosilicates

In 1966 the formation of aluminosilicates in marine environments was hypothesized by Mackenzie and Garrels (1966) who pointed out the potential significance of this process with respect to the oceanic chemistry and for global elemental cycles. As elements are transferred into solid phase and thus become insoluble this process is referred to 'reverse weathering'. Within the scope of this textbook only a brief overview of the major processes and conditions of formation is intended to be outlined.

Four major pathways for the formation of iron bearing aluminosilicates can be distinguished:

1. Formation from weathered basalt and volcanic ashes
2. Glauconite formation
3. Formation in the vicinity of hydrothermal vents
4. Formation under low temperature conditions

The first two pathways of formation will not be discussed here as they were found to be only of local/regional importance and are not considered to be of major importance for early diagenetic reactions. Iron bearing clay mineral formation under high-temperature conditions near a hydrothermal system of the Red Sea was studied by Bischoff (1972). A direct precipitation of an iron-rich smectite (nontronite) within the metalliferous sediments was found. This pathway of clay mineral formation was shown to occur at temperatures

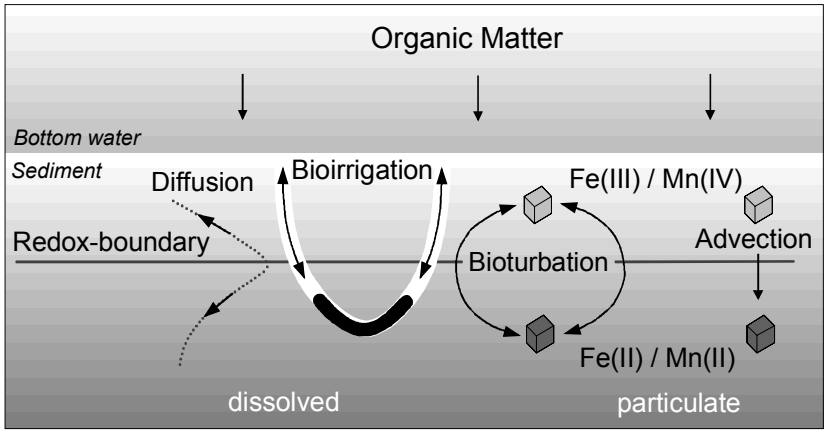

Fig. 7.18 Modes of transport in the sediment: molecular diffusion, bioirrigation, bioturbation, and advection.

typically ranging between 70 and 150 °C under oxic and anoxic conditions (Cole and Shaw 1983). Yet, lowest temperatures of formation were deduced to be ~ 20 °C (McMurtry et al 1983; Singer et al. 1984). Experimental studies by Decarreau et al. (1987) demonstrated the synthesis of dioctahedral smectite, containing Fe(III) within the octahedral sheet, only under strictly oxic conditions.

Experimental results by Harder (1976, 1978) gave evidence for the potential of iron bearing clay mineral formation under low temperature deep-sea floor conditions. Subsequent findings of sediments rich in montmorillonites in the north equatorial Pacific (Hein et al. 1979) and nontronite in the Bauer Deep of the eastern equatorial Pacific (Cole and Shaw 1983; Cole 1985) were attributed to authigenic aluminosilicate formation. For the formation of low-temperature iron-bearing aluminosilicates the deposition of skeletal opal (e.g. radiolarian) and iron oxyhydroxide (e.g. precipitation products of hydrothermal activity) as well as a low carbonate content are considered (Cole and Shaw 1983). Enhanced opal dissolution due to the presence of high iron oxide concentrations were reported (Mayer et al. 1991), yet kinetic reasoning of this observation remains unclear. As the skeletal opal closely associated with the iron oxyhydroxide becomes buried it dissolves and forms an amorphous Fe(III)-silica complex at the skeleton surface which subsequently recrystallizes to form nontronite on the surface of the partially dissolved skeletons (Cole 1985). By this analogy, Harder (1976,1978) also found an amorphous Fe(III)-silicate precipitate as a precursor which developed during aging under suboxic conditions into a crystalline iron-rich clay mineral. The presence of Fe^{2+} was a prerequisite for the synthesis of clay minerals under experimental conditions and therefore partial reduction of iron oxyhydroxide within the microenvironment of an opal skeleton must be assumed. The oxygen isotopic composition ($\delta^{18}O$) of the authigenic mineral can be used to reconstruct the prevailing temperature during formation by applying the geothermometric equation of Yeh and Savin (1977). For the aluminosilicates from the north equatorial Pacific and the Bauer Deep formation temperatures of ~ 3-4 °C were deduced representing authigenic formation under low-temperature conditions in deep-sea sediments. Similar to the above described deep-sea conditions, the Amazon delta represents an iron and silicate rich depositional environment. Incubation experiments with sediments from the Amazon delta revealed substantial K-Fe-Mg-clay mineral formation within 1-3 years under low-temperature conditions (Michalopoulos and Aller 1995) implying significant elemental transfer into solid phase within the estuarine mixing zone.

7.4.4 Iron and Manganese Redox Cycles

Processes of early diagenesis can only be understood by integrating biogeochemical reactions and modes of transport in the sediment. With respect to the quantification of iron and manganese reactions molecular diffusion and bioirrigation need to be considered for the dissolved phase whereas bioturbation and advection are relevant for the particulate transport (Haese 2002). Bioirrigation is the term for solute exchange between the bottom water and tubes in which macro-benthic organisms actively pump water. For iron and manganese a recent study (Hüttel et al. 1998) points out the importance of solute transport in the sediment and across the sediment / bottom water interface due to pressure gradients induced by water flow over a rough sediment topography. Advection in the context of particulate transport describes the downward transport of particles relative to the sediment surface due to sedimentation. Strictly speaking, bioturbation (sometimes more generally termed mixing) also induces a vertical transport of dissolved phase. Yet, as molecular diffusive transport is usually much greater than dissolved transport by bioturbation the later is usually neglected.

The cycling of reduced and oxidized iron and manganese species are discussed together in this chapter since the driving processes are principally the same. In Fig. 7.18 the operating modes of transport are shown schematically along with a redox boundary. Above this boundary the reactive fraction of total solid phase iron or manganese is present as oxidized species whereas below the reduced species occur. Note that at this boundary a build-up in the pore water occurs if no immediate precipitation (e.g. FeS) or adsorption inhibits a release into ambient water. The change in the redox state implies oxidation above and reduction below by some electron donor / acceptor. In case of dissimilatory iron / manganese reduction the organic carbon serves as electron donor, the other most important oxidants and reductants are discussed in the sections 7.4.3.1 and 7.4.3.2 .

The intensity of the redox cycling and thus the importance for oxidation and reduction reactions in the sediment is terminated by either one of the following conditions: 1. In case of the absence of any efficient oxidant (e.g. O_2) in the upper-most layer or bottom water no oxidation will occur and the redox cycling cannot be maintained. 2. In case of the absence of a reactive fraction (bioavailable or 'rapidly' reducible by HS^-, see section 7.4.3.1) in the lower layer no reduction will occur and the redox cycle will cease. 3. A vertical transport mode must be maintained between the zone of oxidation and the zone of reduction. As advection is usually very much slower than the downward transport by bioturbation the intensity of bioturbation terminates the transport between the redox-zones.

For the most simple assumption of an homogeneously mixed layer the intensity of bioturbation is expressed by the biodiffusion (or mixing) coefficient, D_b, which can be deduced appropriately along with the sedimentation rate with the aid of natural radioactive isotopes. According to Nittrouer et al. (1983/1984) the general advection-diffusion equation can be rearranged to calculate the sedimentation rate, A:

$$A = \frac{\lambda x}{\ln \frac{C_0}{C_x}} - \frac{D_b}{x}\left(\ln \frac{C_0}{C_x}\right) \qquad (7.17)$$

with λ: decay constant [y^{-1}], x: depth interval between two levels [cm], C_0, C_x: activity at an upper sediment level and at a lower level with the distance x below C_0 [decays per minute, dpm] D_b: biodiffusion coefficient [$cm^2\ y^{-1}$]. If mixing is negligible ($D_b = 0$) then the above equation can be simplified:

$$A = \frac{\lambda x}{\ln \frac{C_0}{C_x}} \qquad (7.18)$$

In case of a very low sedimentation rate relative to mixing ($A^2 \ll \lambda \cdot D_b$) Eq. 7.17 can be rearranged to calculate the biodiffusion coefficient, D_b:

$$D_b = \lambda \left(\frac{x}{\ln \frac{C_0}{C_x}} \right)^2 \qquad (7.19)$$

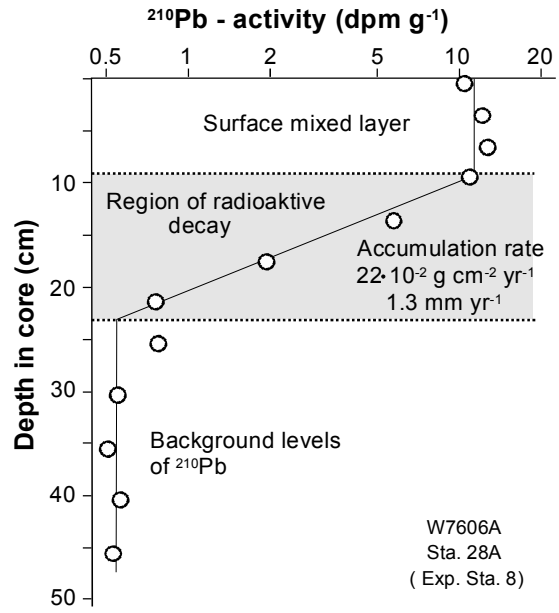

Fig. 7.19 ^{210}Pb-activity depth profile from the Washington shelf (adopted from Nittrouer 1983/1984). The sediment surface layer is mixed as can be deduced from homogenous ^{210}Pb values. Below, constantly decreasing values imply no or hardly any mixing, this gradient can be used to calculate a sedimentation rate. The deepest part is characterized by a homogenous background activity resulting from the decay of ^{226}Ra in the sediment.

The above restrictions for the calculations of the sedimentation rate and the biodiffusion coefficient imply the use of radioactive isotopes with different half-lifes ($t_{1/2} = 0.693 \cdot \lambda^{-1}$) for different purposes and depositional environments. The higher the sedimentation rate, the shorter should be the half-life of the radioactive isotope. The more intense bioturbation in the surface layer, the shorter should be the half-life of the applied radioactive isotope be. For coastal and shelf sediments sedimentation rates of several decimeters to few meters per 1000 years are typical and can be determined by ^{210}Pb ($t_{1/2}$ = 22.3 y). Shorter lived isotopes (e.g. $t_{1/2}$ of ^{234}Th = 24.1 d) are applicable for the determination of the mixing intensity. ^{230}Th ($t_{1/2}$ = 75,200 y) is a commonly used radioactive isotope in oceanographic sciences to trace processes over longer periods of times. The above isotopes are rapidly scavenged by particles once they are formed from the decay of some parent isotopes and settle to the sea floor. Due to analytical reasons post-depositional processes can be traced for a time

period of 4 to 5 times of the radioactive half-life which is approximately 100 years in case of ^{210}Pb.

In Figure 7.19 a typical ^{210}Pb-activity depth profile from the Washington shelf is shown. The uppermost 9 cm are characterized by constant ^{210}Pb activity implying intensive mixing in the surface layer. Below, ^{210}Pb activity decreases linearly (on a log-scale) indicating no mixing and continuous decay. The lowest part of the profile is characterized by constantly very low values resulting from the long-term decay of ^{226}Ra to ^{210}Pb in the sediment. This background value is subtracted from the above activities, which are then termed excess-^{210}Pb or unsupported-^{210}Pb. The depth interval showing a linear decrease on a log-activity scale is often used to calculate a sedimentation rate. Yet, a strong overestimation of the true sedimentation rate is possible as slight deep bioturbation in this part may not be seen exclusively by ^{210}Pb as it was shown by Aller and DeMaster (1984). The investigation of an additional, shorter-lived isotope within this depth interval will reveal a potential influence of bioturbation.

As mentioned in the beginning of this section bioturbation and advection by sedimentation cause particle transport in the sediment. In Fig. 7.20 three scenarios are schematically shown representing constant molecular diffusive and advective transport while bioturbation varies. As a result, the shape of the solid phase profile varies distinctively. In case of no bioturbation the molecular diffusive flux ($J_{diff.}$) from the zone of dissolution into the zone of precipitation causes a thin, sharp peak (enrichment) (Fig. 7.20a) whereas slight bioturbation and thus vertical up- and down-transport of particles (J_p) broadens the enrichment (Fig. 7.20b). In case of very intense particle transport relative to the molecular diffusive transport ($J_{p.} \gg J_{diff.}$, Fig. 7.20c) hardly any or no enrichment will be formed although a distinctive depth of precipitation is still present. In summary, we can conclude that the solid phase profile is a result of the dissolution within the lower part of the enrichment, as well as of the sedimentation rate and of the bioturbation (mixing) intensity. This can be expressed mathematically by a one-dimensional transport-reaction model according to Aller (1980). If bioturbation and sedimentation with depth (no compaction) are constant, steady-state conditions apply (chapter 3), and solid phase decreases linearly over the interval of dissolution, then

$$P = -\frac{(C_1 - C_2)}{(x_2 - x_1)} \cdot D_b + A \cdot (C_1 - C_2) \qquad (7.20)$$

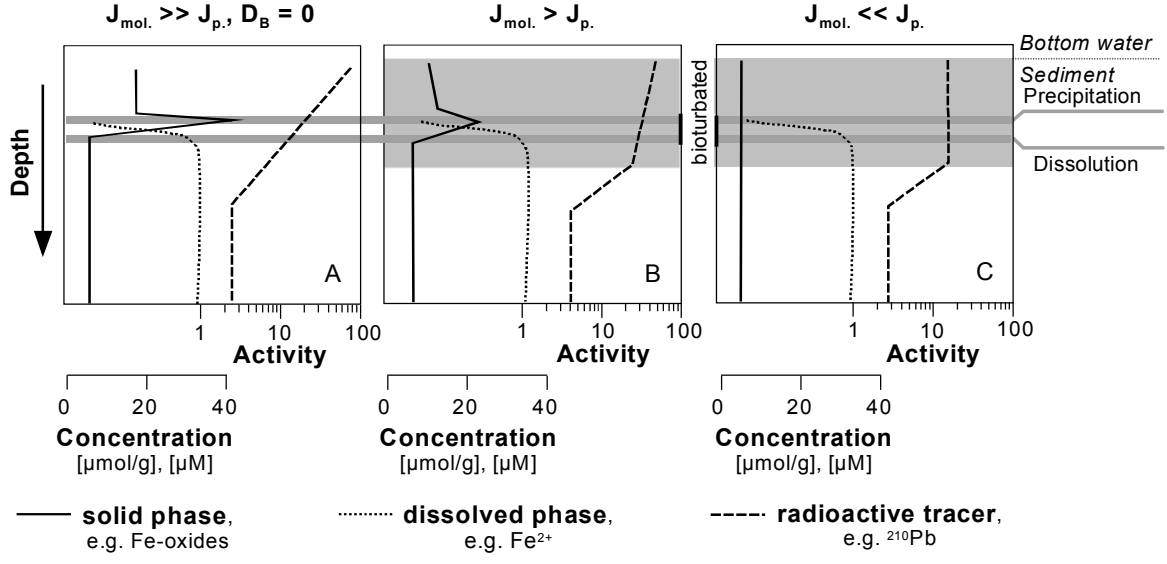

Fig. 7.20 To illustrate the influence of bioturbation (mixing) on the solid phase profile three schematic scenarios are drawn. For all scenarios the same molecular diffusive transport ($J_{mol.}$) and sedimentation is assumed, yet the particulate transport ($J_{p.}$) by bioturbation is varied. A: As no bioturbation occurs a distinctive, thin solid phase enrichment is formed in the zone of precipitation. B: The enrichment broadens up- and downwards as slight bioturbation is present. C: In case of a much higher particulate transport relative to the diffusive transport ($J_p \gg J_{mol.}$) hardly any enrichment will be formed.

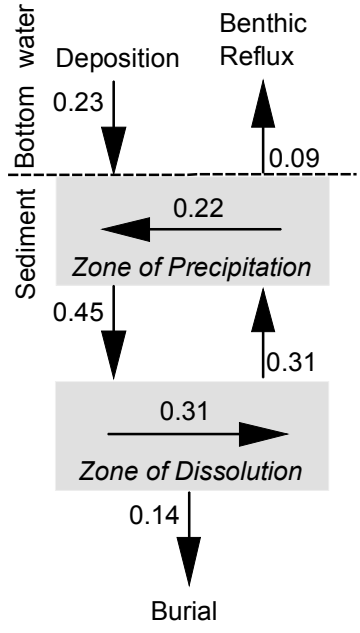

Fig. 7.21 Example of manganese cycling across the sediment/bottom water interface and within the sediment (modified after Sundby and Silverberg (1985). The applied depth-dependent flux model is described in the text. Depositional, burial, and molecular diffusive fluxes as well as the reduction rate within the zone of dissolution were calculated independently.

can be calculated according to Sundby and Silverberg (1985). P resembles the production (or dissolution) rate and the other variables are according to Eq. 7.17 except that C is given as concentration per volume [µmol cm^{-3}] as the depth distribution of solid phase strongly depends on the porosity.

In addition to the dissolution rate one can calculate the burial rate of non-reactive phase and the input rate to the sediment surface once the sedimentation rate is known. Based on these independently calculated fluxes Sundby and Silverberg (1985) developed a depth-zonated flux model for manganese in the St. Lawrence estuary. Their depth-dependent reactive zones were surface water, bottom water, sediment depth of precipitation (oxidation), sediment depth of dissolution (reduction) and depth of eventually buried sediment. One example of their Mn-cycling results is given in Fig. 7.21.

The cycling of elements in bioturbated surface sediments can also be expressed in terms of turnover times defined as period of time required for a complete oxidation - reduction cycle of the reactive fraction. Additional consideration of the bioturbation depth and the sedimentation rate then reveals the number of redox-cycles before ultimate burial. In Tab. 7.2 representative results for estuarine (coastal) and slope sediments are given.

7.4.5 Discussion: The Importance of Fe- and Mn-Reactivity in Various Environments

The above sections of this chapter have shown the high variability of iron-input modes, fluxes and reactivity towards oxidized and reduced species in marine sediments. Within this section the importance of iron and manganese reactivity with respect to the mineralization of organic matter as well as to the chemical oxidation (reduction) of reduced (oxidized) species within different depositional environments will be discussed and hopefully inspire further considerations.

In order to investigate the importance of iron and manganese reduction and oxidation processes one needs to determine their rates and compare

Table 7.2 Calculated turn-over times and times of redox cycling before burial in coastal and slope sediments. The dynamic of redox cycling becomes evident by envisaging a complete oxidation - reduction cycle on a 2 - 6 months time scale.
([1] Sundby and Silverberg 1985, [2] Aller 1980, [3] Canfield et al. 1993a, [4] Thamdrup and Canfield 1996)

Location	Fe/Mn	Turn-over time [d]	Times cycled before burial
St. Lawrence estuary [1]	Mn	43 - 207	
Long Island Sound estuary [2]	Mn	60 - 100	
Skagerrak [3]	Fe/Mn	70 - 250	130 - 300
Slope off Chile [4]	Fe	70	31 - 77

Table 7.3 Summary of results quantifying the relative contribution of dissimilatory iron and manganese reduction for the decomposition of organic matter.
([1] Wang and Van Cappellen 1996, [2] Canfield et al. 1993b, [3] Canfield et al. 1993a, [4] Aller 1990, [5] Thamdrup and Canfield 1996).

Location		Net-Fe/Mn deposition [µmol $cm^{-2}y^{-1}$]	Biodiff. coeff. [$cm^{-2}y^{-1}$]	Dissimilatory Fe/Mn reduction [%]	Total org. C decomposition [%]
Skagerrak, S4/S6	Fe	6 - 14 [3]	80 - 87 [2]		32 - 51 [2]
	Fe	13 - 24 [1]		71 - 84 [1]	
	Mn	1 - 15 [1]		3 - 24 [1]	0 [2]
Skagerrak, S9	Mn	5 - 10 [3]	19 [2]		90 [2]
	Mn	13 [1]		100 [1]	
	Fe	14 [1]		0 [1]	0 [2]
Panama Basin [4]	Mn	'high'	100	100	100
Cont. Slope Chile [5]	Fe	5.1	9; 29	46; 84	12; 29

these with other early diagenetic reaction pathways. For example, rates of organic carbon mineralization by each electron acceptor (O_2, NO_3^-, Mn(IV), Fe(III), SO_4^{2-}) are - strictly speaking - necessary to make a statement on the relative contribution of dissimilatory iron and manganese reduction. For the case of iron and manganese, the determination of such rates are problematic as both electron acceptors may be reduced by reduced species as well as by microbial respiration. Additionally, pore water fluxes usually strongly underestimate the true reduction rate as adsorption and precipitation of Fe^{2+}/Mn^{2+}-bearing minerals buffer the build-up within pore-water. Therefore, 'rates of dissimilatory Fe-oxide and Mn-oxide reduction are the least well quantified of the carbon oxidation pathways' (Canfield 1993).

An overview of methods to determine the various organic carbon oxidation pathways is provided by Canfield (1993). As these methods are technically highly demanding and time-consuming, only very few sediments have been investigated with respect to the contribution of the different organic carbon oxidation pathways. Among such studies different methods have been applied which may bear additional uncertainties. Thus, a present-day discussion on the importance of iron and manganese must be speculative to some degree. In Table 7.3 results of different studies concerning the relative contribution of dissimilatory iron and manganese reduction are summarized.

Notice that the results by Wang and Van Capellen (1996) are model results for which some results of Canfield et al. (1993 a,b) were used for the basic data set. A comparison of different locations reveals significant variabilities in the biodiffusion coefficient. For open ocean sediments one can expect even much lower deposition rates and biodiffusion coefficients. Similarly, the proportion of dissimilatory reduction (relative to dissimilatory plus chemical reduction) as well as the proportion of organic carbon mineralization by iron and manganese reduction (relative to total organic carbon oxidation) varies significantly.

The above sites of investigation are distinct by different depositional environments. Skagerrak sediments were retrieved from water depths of 200 (S4), 400 (S6), and 700 (S9) meters and site S9 is located in the central Norwegian Trough where solid phase manganese content made up to 3.5 - 4 wt%. The Panama Basin site is ~ 4000 m deep and is located in the equatorial upwelling region as well as in the vicinity of hydrothermal activity causing a delivery of large amounts of reactive organic matter and manganese to the sea floor. Sites from the continental slope off Chile were investigated during a period of intense upwelling. The intensity of redox-cycling is controlled by the intensity of bioturbation, the input and reduction of reactive Fe(III)/Mn(IV), as well as by the oxidation rate (section 7.4.4). Yet, Fe- and Mn-cycling may only become quantitatively signi-

ficant if reduction is predominantly coupled to dissimilation and chemical reduction is unimportant. This is the case for the manganese dominated sites Skagerrak S9 and Panama Basin where neither the production of HS^- nor of Fe^{2+} was found. O_2 consumption was (almost) completely attributed to the reoxidation of Mn^{2+} in these cases. In contrast, Skagerrak sites S4 and S6 as well as sediments off Chile resemble situations where iron is reduced chemically (HS^-) by up to ~ 50 % and only smaller amounts of ferric iron are available for the dissimilation. A third situation can be inferred for typical open ocean sediments where low Fe/Mn and organic matter deposition along with low bioturbation intensity occurs. Here organic matter decomposition is restricted to aerobic respiration and denitrification. Iron and manganese reduction rates are presumably negligible, yet over a long period of time a significant proportion of manganese is redistributed and the composition of iron oxide phases changes (Haese et al. 1998).

An extensive study in a shallow water, estuarine mixing zone elucidated ideal conditions for efficient manganese cycling (Aller 1994). Manganese turn-over was found to be most intense during warm periods with intensive bioturbation, well-oxygenated bottom water, and moderate organic matter input. Under such conditions manganese reoxidation consumed 30-50 % of the benthic oxygen flux and manganese reduction was mainly induced by HS^-, FeS and FeS_2. As soon as bottom water became O_2-depleted the sedimentary Mn-cycle was reduced as dissolved Mn escaped out of the sediment. The influence of bioirrigation has not yet been explicitly investigated but modeling results by Wang and Van Capellen (1996) imply enhanced metal cycling efficiency with increasing irrigation due to more rapid Fe^{2+}- / Mn^{2+}-oxidation.

A conceptual model describing the importance of iron and manganese reactivity in different environments is only sketchy as results are scarce and manifold aspects deserve further investigations. A general complication concerns the differentiation of dissimilatory and chemical reduction of Mn-oxide when concurrent iron reduction is apparent and further investigations need to discriminate each reaction pathway. The reactivity of smectite-bound iron has only been shown qualitatively (Kostka et al. 1996; König et al. 1997), yet quantifications with respect to dissimilatory and/or chemical reactions are missing. An important role of adsorbed Fe^{2+} / Mn^{2+} is indicated (Sørensen and Thorling 1991; Roden and Zachara 1996) but not proved by sediment studies. Investigations focusing on the importance of metal cycling and its influence on pathways of organic matter decomposition are scarce (Canfield et al. 1993a, Wang and Van Capellen 1996), yet necessary to understand an important link of the carbon cycle.

7.5 The Assay for Ferric and Ferrous Iron

In order to study iron reactivity qualitatively and quantitatively it is essential to quantify the ferrous and ferric iron fractions of the present minerals or mineral groups. With respect to the determination of iron speciation the principal problem is the rapid oxidation of ferrous iron. Atmospheric oxygen diffuses into pore water where it oxidizes dissolved ferrous iron 'immediately' and starts oxidizing FeS and FeS_2. Reduced smectites may also become oxidized under air atmosphere within hours. Therefore, if dissolved iron and iron speciation of solid phase are to be determined samples need to be conserved under inert gas atmosphere. No extra care is needed for the determination of total iron of solid phase.

Above a pH of 3 and in the absence of chelators dissolved iron is only present as ferrous iron under natural conditions. Therefore, the colored complex that results from the reaction between ferrous iron and a reagent can be analysed colorimetrically and correlates with the concentration of total dissolved iron. Most conveniently, one can mix a drop of Ferrozine® solution (Stookey 1970), one drop of H_2SO_4 (diluted 1:4) and 1 ml of pore water in the glove box, wait until complex formation is completed (20-30 minutes) and quantify the iron concentration by the intensity of the color at a wavelength of 562 nm. To avoid matrix effects standards should be prepared with artificial seawater.

The assay of solid phase ferrous and ferric iron has a long tradition due to the early interest in soil chemistry. Publications on extraction / leaching conditions and results from varying soils and sediments are extensive and thus, within the scope of a textbook, only important principals and a description of the (subjectively) most important extractions can be given. Since a

great variety of the quantitatively most important iron bearing minerals / mineral groups is present in marine sediments a series of different extractions is necessary in order to achieve a complete distribution of ferrous and ferric iron. In general, the extraction conditions applied to natural sediments result from experiments conducted in advance proving the dissolution of individual minerals or mineral groups. Because the grain size, degree of crystallinity, ionic substitution within minerals and varying matrix constituents influence the dissolution kinetics during the extraction a clear-cut mineral specific determination is usually not possible with this approach. Yet, extractions have been successfully applied to show patterns of mineral (group) dissolution and precipitation and to deduce reaction rates. For a comparison with results of other studies exactly

Table 7.4 Solubility of iron bearing minerals derived under experimental conditions. + / - imply a solubility of ≥ 97 % / ≤ 3 %, values indicate a percentage of release.

(1) Schwertmann (1964): 0.2 M NH_4^+-oxalate / 0.2 M oxalic acid; pH: 2.5, 2 h in darkness
(2) Ferdelman (1988): 10 g Na-citrate + 10 g Na-bicarbonate mixed in 200 ml distilled and deionized water, deaerated, before 4 g ascorbic acid are added; pH: 7.5, 24 h
(3) Lord (1980): 0.35 M acetate / 0.2 M Na-citrate + 1.0 g Na-dithionite for each sample (~ 1 g wet sediment in 20 ml solution); pH: 4.8, 4 hours.
(4) Chao and Zhou (1983): 1 M HCl, 30 min; Canfield (1988): 1 M HCl 20-23 h; Cornwell and Morse (1987): 1 M HCl, 45 min; Kostka and Luther (1994): 0.5 M, 1 h.
(5) Haese et al. (1997): 1 ml distilled and deionized water + 1 ml conc. H_2SO_4 + 2 ml HF were added to ~ 250 mg of wet sediment under inert gas atmosphere and constant stirring over few minutes.
(6) Canfield et al. (1986): 15 ml of O_2-free 1 M $CrCl_2$ in 0.5 M HCl + 10 ml of 12 M HCl under inert gas atmosphere.

(a) Chou and Zhou 1983, (b) Canfield 1988, (c) Kostka and Luther 1994, (d) Ruttenberg 1992, (e) Mehra and Jackson 1960, (f) Cornwell and Morse 1987, (g) Haese et al. 1997, (h) Canfield et al. 1986.

Mineral	Oxalate (1)	Ascorbate (2)	Dithionite (3)	HCl (4)	HF/H_2SO_4 (5)	Cr(II)/ HCl (6)
am. $Fe(OH)_3$	+ (a)			34 - 72 (a) + (b)		
Ferrihydrite	+ (b)	+ (c)	+ (b,c,d)	+ (b,c)		
Lepidocrocite	+ (b)		+ (b)	7 (b)		
Goethite	- (a,b)	- (c)	91 (c) + (b)	- (a,b,c)	+ (g)	
Hematite	- (a,b)	- (c)	63 (c) + (b,d,e)	- (a,b,c)	+ (g)	
Magnetite	60 (c)	- (c)	90 (c) - (b)	- (a,b,c)	+ (g)	
(am.) FeS	+ (c)			+ (f)		+ (h)
Pyrite (FeS_2)				- (b,f)		+ (h)
Chlorite	- (b,c)	- (c)	5 - 7 (c,b)	27 (c) 32 (b)	10 - 100 (g)	
Nontronite	- (b)		27 (b)	7 (b)		
Glauconite	- (b)		10 (b)	10 (b)		
Garnet	- (b)		- (b)	- (b)		

the same extraction conditions (reagent composition, sediment : solution ratio, contact time) must be applied.

Table 7.4 gives an overview of experimentally derived dissolution behavior of iron bearing minerals under some selected extraction conditions. The investigation of total-Fe from ascorbate and dithionite solution can be determined by ICP-AES or flame-AAS. Ferrous and ferric iron from non-reducing or non-oxidizing extractions can be determined by polarographic methods (Wallmann et al. 1993) or colorimetrically with and without the addition of a reducing agent (e.g. hydroxylamine hydrochloride, Kostka and Luther 1994). During the acidic extractions evolving sulfide can be trapped in a separate alkaline solution (e.g. Sulfur Antioxidant Buffer, SAOB, Cornwell and Morse 1987) where it can be determined polarographically, by precipitation titration with Pb or by a standard ion sensitive electrode. Sulfide evolving from HCl extraction is called Acid Volatile Sulfur (AVS).

The leaching with HF/H_2SO_4 as described above and the subsequent polarographic determination of ferrous and ferric iron is based on work by Beyer et al. (1975) and Stucki (1981) in order to quantify the silicate bound ferrous and ferric iron. This extraction has hardly been applied with respect to questions of early diagenesis so far, yet, the silicate bound iron fraction is quantitatively very important in marine sediments and even a small reactive fraction of this pool may be of overall significance for the iron reactivity. As a complementary method to the commonly applied extractions (Table 7.4) it renders the calculation of the total iron speciation in the sediment which may then be compared to Mössbauer-spectroscopic results (Haese et al. 1997; Haese et al. 2000).

One of the pitfalls in the interpretation of extraction results from natural sediments is caused by the fact that the presence of Fe^{2+} complexed by carboxylic acid catalyzes the reduction of crystalline iron oxides such as hematite (Sulzberger et al. 1989), magnetite (Blesa et al. 1989) and goethite (Kostka and Luther 1994). In order to avoid this catalytic dissolution of well-crystallized iron oxides by Fe^{2+} during the oxalate extraction Thamdrup and Canfield (1996) air-dried the sediment in advance, thereby oxidizing FeS and $FeCO_3$ to ferrihydrite. In addition, they applied the anoxic oxalate extraction and subtracted the released amount of Fe^{2+} from the amount of Fe^{3+} determined from the oxic extraction to calculate the poorly crystallized iron oxide fraction as intended according to Table 7.2.

Acknowledgements
I wish to thank Tim Ferdelman, Bo Thamdrup and Caroline Slomp for their critical reviews in the year 2000 leading to the first edition of this manuscript. The recent edition was improved by comments by Lynda Radke and Emmanuelle Grosjean, and it received permission for publication by the Chief Executive Officer of Geoscience Australia.

7.6 Problems

Problem 1

The Burdekin River is large river in northwestern Australia, which discharges about 3.4 million tons of sediment into the coastal sea.
a) Estimate how much total and highly reactive iron is discharged from the catchments. Assume that the sediment is of average continental crust composition. b) Estimate how much highly reactive iron remains in the estuary and in the near-coastal zone. c) Which other source of iron must be considered off-shore of northern Australia?

Problem 2

a) List 3 mineral properties of iron oxyhydroxides which influence the rate of microbial iron reduction. b) Explain why wet-chemical extractions are not mineral specific.

Problem 3

Explain why bioturbation is important for the rate of dissimilatory iron reduction in sediments.

Problem 4

Which are important variables affecting the importance of dissimilatory Fe- and Mn-reduction relative to other metabolic pathways?

Problem 5

a.) Define and explain the abbreviation DOP.
b.) Which extractions are used to determine DOP.

References

Aller, R.C., 1980. Diagenetic processes near the sediment-water interface of Long Island Sound. 2. Fe and Mn. Advances in Geophysics, 22: 351-415.

Aller, R.C. and DeMaster, D.J., 1984. Estimates of particle flux and reworking at the deep-sea floor using $^{234}Th/^{238}U$ disequilibrium. Earth and Planetary Science Letters, 67: 308-318.

Aller, R.C., 1990. Bioturbation and manganese cycling in hemipelagic sediments. Philosophical Transactions of the Royal Society of London A, 331: 51-68.

Aller, R.C., 1994. The sedimentary Mn cycle in Long Island Sound: Its role as intermediate oxidant and the influence of bioturbation, O_2, and C_{org} flux on diagenetic reaction balances. Journal of Marine Research, 52 (2): 259-295.

Balzer, W., 1982. On the distribution of iron and manganese at the sediment/water interface: thermodynamic vs. kinetic control. Geochimica Cosmochimica Acta, 46: 1153-1161.

Bell, P.E., Mills, A.L. and Herman, J.S., 1987. Biogeochemical conditions favoring magnetite formation during anaerobic iron reduction. Applied and Environmental Microbiology, 53: 2610-2616.

Berger, W.H., Smetacek. V.S. and Wefer, G., 1989. Ocean productivity and paleoproductivity - An overview. In: Berger, W.H., Smetacek, V.S. and Wefer, G. (eds), Productivity of the oceans: present and past. John Wiley and Sons, Chichester, 1-34.

Berner, R.A., 1970. Sedimentary pyrite formation. American Journal of Science, 268: 1-23.

Berner, R.A., 1971. Principles of chemical sedimentology. McGraw-Hill, New York., 240 pp.

Beyer, M.E., Bond, A.M. and McLaughlin, R.J.W., 1975. Simultaneous polarographic determination of ferrous, ferric and total iron in standard rocks. Analytical Chemistry, 47 (3): 479-482.

Biber, M.V., Dos Santos Afonso, M. and Stumm, W., 1994. The coordination chemistry of weathering: IV: Inhibitation of the dissolution of oxides minerals. Geochimica Cosmochimica Acta, 58 (9): 1999-2010.

Bischoff, J.L., 1972. A ferroan nontronite from the Red Sea geothermal system. Clays and Clay Minerals, 20: 217-223.

Blank, M., Leinen, M. and Prospero J.M., 1985. Major Asian aeolian inputs indicated by the mineralogy of aerosols and sediments in the western North Pacific. Nature, 314: 84-86.

Blesa, M.A., Marinovich, H.A., Baumgartner, E.C., and Marota, A.J.G., 1987. Mechanism of dissolution of magnetite by oxalic acid - ferrous ion solution. Inorganic Chemistry, 26: 3713-3717.

Böhm, J., 1925. Über Aluminium- und Eisenoxide I. Zeitschrift der Anorganischen Chemie, 149: 203-218.

Bonneville, S., Van Cappellen, P., and Behrends, T., 2004. Microbial reduction of iron(III) oxyhydroxides: effects of mineral solubility and availability. Chemical Geology, 212: 255-268.

Borer, P.M., Sulzberger, B., Reichard, P., and Kraemer, S.M., 2005. Effect of siderophores on the light-induced dissolution of colloidal iron(III) (hydr)-oxides. Marine Chemistry, 93: 179-193.

Broecker, W.S., Spencer, D.W., Craig, H., 1982. GEOSECS Pacific Expedition: Hydrographic Data. U.S. Goverment Printing Office, Washington, DC, 3: 137 pp.

Bruland, K.W., Rue, E.L., Smith, G.J., and DiTullio, G.R., 2005. Iron, macronutrients and diatom blooms in the Peru upwelling regime: brown and blue waters of Peru. Marine Chemistry, 93: 81-103.

Buresh, R.J. and Moraghan, J.T., 1976. Chemical reduction of nitrate by ferrous iron. Journal of Environmental Quality, 5: 320-325.

Canfield, D.E., Raiswell, R., Westrich, J.T., Reaves, C.M. and Berner, R.A., 1986. The use of chromium reduction in the analysis of reduced inorganic sulfur in sediments and shales. Chemical Geology, 54: 149-155.

Canfield, D.E., 1988. Sulfate reduction and the diagenesis of iron in anoxic marine sediments. Ph.D. thesis. Yale Univ., 248 pp.

Canfield, D.E., 1989. Reactive iron in marine sediments. Geochimica Cosmochimica Acta, 51: 619-632.

Canfield, D.E., Raiswell, R. and Botrell, S., 1992. The reactivity of sedimentary iron minerals towards sulfide. American Journal of Science, 292: 659-683.

Canfield, D.E., 1993. Organic matter oxidation in marine sediments. In: Wollast, R., Mackenzie, F.T. and Chou, L. (eds) Interactions of C, N, P and S biogeochemical cycles and global change. NATO ASI Series, 4, Springer, Berlin, Heidelberg, NY, pp. 333-363.

Canfield, D.E., Thamdrup, B. and Hansen, J.W., 1993a. The anaerobic degradation of organic matter in Danish coastal sediments: Iron reduction, manganese reduction, and sulfate reduction. Geochimica Cosmochimica Acta, 57: 3867-3883.

Canfield, D.E., Jørgensen, B.B., Fossing, H., Glud, R., Gundersen, J., Ramsing, N.B., Thamdrup, B., Hansen, J.W., Nielsen, L.P. and Hall, P.O.J., 1993b. Pathways of organic carbon oxidation in three continental margin sediments. Marine Geology, 113: 27-40.

Canfield, D.E., 1997. The geochemistry of river particles from the continental USA: Major elements. Geochimica Cosmochimica Acta, 61: 3349-3365.

Carlson, T.N. and Prospero, J.M., 1972. The large-scale movement of Saharan air outbreaks over the northern equatorial Atlantic. Journal of Applied Meteorology, 11: 283-297.

Carothers, W.W., Adami, L.H. and Rosenbauer, R.J., 1988. Experimental oxygen isotope fractionation between siderite-water and phosphoric acid liberated CO_2-siderite. Geochimica Cosmochimica Acta, 52: 2445-2450

Chavez, F.P. and Barber, R.T., 1987. An estimate of new production in the equatorial Pacific. Deep Sea Research, 34: 1229-1243.

Chester, R., 1990. Marine Geochemistry. Chapman & Hall, London, pp. 698.

Chou, T.T. and Zhou, L., 1983. Extraction techniques for selective dissolution of amorphous iron oxides from soils and sediments. Soil Science Society American Journal, 47: 225-232.

Cole, T.G. and Shaw, H.F., 1983. The nature and origin of authigenic smectites in some recent marine sediments. Clay Minerals, 18: 239-252.

Cole, T.G., 1985. Composition, oxygen isotope geochemistry, and the origin of smectite in the metalliferous sediments of the Bauer Deep, southeast Pacific. Geochimica Cosmochimica Acta, 49: 221-235.

Coleman, M.L., Hedrick, D.B., Lovley, D.R., White, D.C. and Pye, K., 1993. Reduction of Fe(III) in sediments by sulphate-reducing bacteria. Nature, 361: 436-438.

Cornwell, J.C. and Morse, J.W., 1987. The characterization of iron sulfide minerals in anoxic marine sediments. Marine Chemistry, 22: 193-206

Crosby, S.A., Glasson, D.R., Cuttler, A.H., Butler, I., Turner, D.R., Whitfield, M. and Millward, G.E., 1983. Surface areas and porosities of Fe(III)-Fe(II)-derived oxyhydroxides. Environmental Science and Technology, 17: 709-713.

De Angelis, M., Barkov, N.I., Petrov, V.N., 1987. Aerosol concentrations over the last climatic cycle (160 kyr) from Antarctic ice core. Nature, 325: 318-321.

De Baar, H.J.W. and Suess, E., 1993. Ocean carbon cycle and climate change - An introduction to the interdisciplinary union symposium. Global and Planetary Change, 8: VII-XI.

Decarreau, A., Bonnin, D., Badauth-Trauth, D., Couty, R. and Kaiser, P., 1987. Synthesis and crystallogenesis of ferric smectite by evolution of Si-Fe coprecipitates in oxidizing conditions. Clay Minerals, 22: 207-223.

Donaghay, P.L., 1991. The role of episodic atmospheric nutrient inputs in chemical and biological dynamics of oceanic ecosystems. Oceanography, 4: 62-70.

Dos Santos Afonso, M. and Stumm, W. 1992, Reductive dissolution of iron(III)(hydr)oxides by hydrogen sulfide. Langmuir, 8: 1671-1676.

Duce, R.A., Liss, P.S., Merill, J.T., Atlas, E.L., Buat-Menard, P., Hicks, B.B., Miller, J.M., Prospero, J.M., Arimoto, T., Church, T.M., Eillis, W., Galloway, J.N., Hansen, L., Jickells, T.M., Knap, A.H., Reinhardt, K.H., Schneider, B., Soudine, A., Tokos, J.J., Tsunogai, S., Wollast, R. and Zhou, M., 1991. The atmospheric input of trace species to the world ocean. Global Biogeochemical Cycles 5: 193-259.

Ehrenreich, A. and Widdel, F., 1994, Anaerobic oxidation of ferrous iron by purple bacteria, a new type of phototrophic metabolism. Applied and Environmental Microbiology, 60: 4517-4526.

Ellwood, B.B., Chrzanowski, T.H., Hrouda, F., Long, G.J. and Buhl, M.L., 1988. Siderite formation in anoxic deep-sea sediments: A synergetic bacterially controlled process with important implications in paleomagnetism. Geology, 16: 980-982

Ferdelman, T.G., 1980. The distribution of sulfur, iron, manganese, copper, and uranium in a salt marsh sediment core as determined by a sequential extraction method. Masters thesis, University Delaware.

Figuères, G., Martin, J.M. and Meybeck, M., 1978. Iron behaviour in the Zaire estuary. Netherlands Journal of Sea Research, 12 (3/4): 329-337.

Froelich, P.N., Klinkhammer, G.P., Bender, M.L., Luedtke, N.A., Heath, G.R., Cullen, D., Dauphin, P., Hammond, D. and Hartman, B., 1979. Early oxidation of organic matter in pelagic sediments of eastern equatorial Atlantic: suboxic diagenesis. Geochimica Cosmochimica Acta, 43: 1075-1090.

Froelich, P.N., Bender, M.L., Luedtke, N.A., Heath, G.R. and DeVries, T., 1982. The marine phosphorus cycle. American Journal of Science, 282: 474-511.

GESAMP (Group of Experts on the Scientific Aspects of Marine Pollution), 1987. Land/sea boundary flux of contaminants: Contributions from rivers. GESAMP Rep. Stud., 32: 172 pp.

Gingele, F., 1992. Zur klimaabhängigen Bildung biogener und terrigener Sedimente und ihre Veränderung durch die Frühdiagenese im zentralen und östlichen Südatlantik (in German). Berichte, 26, Fachbereich Geowissenschaften, Universität Bremen, 202 pp.

Goldberg, S. and Sposito, G., 1984. A chemical model of phosphate adsorption by soils. I. Reference oxide minerals. Soil Scienc Society American Journal, 48: 772-778.

Haese, R.R., Wallmann, K., Kretzmann, U., Müller, P.J. and Schulz, H.D., 1997. Iron species determination to investigate the early diagenetic reactivity in marine sediments. Geochimica Cosmochimica Acta, 61 (1): 63-72.

Haese, R.R., Petermann, P., Dittert, L. and Schulz, H.D., 1998. The early diagenesis of iron in pelagic sediments - a multidisciplinary approach. Earth and Planetary Science Letters, 157: 233-248.

Haese, R.R., Schramm, J., Rutgers van der Loeff, M.M. and Schulz, H.D., 2000. A comparative study of iron and manganese diagenesis in continental slope and deep sea basin sediments off Uruguay (SW Atlantic). International Journal of Earth Sciences, 88: 619-629.

Haese, R.R., 2002. Macrobenthic activity and its effects on biogeochemical reactions and fluxes, In: Wefer, G., Billet, D., Hebbeln, D., Jørgensen, B.B., Schlüter, M. and van Weering, T.C.E. (eds), Ocean margin systems, Springer-Verlag, Heidelberg-Berlin, 219-234.

Harder, H., 1976. Nontronite synthesis at low temperatures. Chemical Geology, 18: 169-180

Harder, H., 1978. Synthesis of iron layer silicate minerals under natural conditions. Clays and Clay Minerals, 26: 65-72.

Hart, T.J., 1934. On the phytoplankton of the south-west Atlantic and the Bellinghausen Sea, 1929-31. Discovery Reports VIII.

Hein, J.R., Yeh, H.-W. and Alexander, E., 1979. Origin of iron rich montmorillonite from the manganese nodule belt of the north equatorial Pacific. Clays and Clay Mineralogy, 27: 185-194.

Hunter, K.A., 1983. On the estuarine mixing of dissolved substances in relation to colloid stability and surface properties. Geochimica Cosmochimica Acta, 47: 467-473.

Hüttel, M., Ziebis, W., Forster, S. and Luther, G.W. III, 1998. Advective transport affecting metal and nutrient distributions and interfacial fluxes in permeable sediments. Geochimica Cosmochimica Acta, 62: 613-631.

Hyacinthe, C., and Van Cappellen, P., 2004. An authigenic iron phosphate phase in estuarine sediments: composition, formation and chemical reactivity. Marine Chemistry, 91: 227-251.

Jensen, H.S., Mortensen, B.P., Andersen, F.Ø., Rasmussen, E. and Jensen, A., 1995. Phosphorus cycling in a coastal marine sediment, Aarhus Bay, Denmark. Limnology and Oceanography, 40: 908-917.

Johnson, K.S., Coale, K.H., Elrod, V.A. and Tindale, N.W., 1994. Iron photochemistry in seawater from the equatorial Pacific. Marine Chemistry, 46: 319-334.

Johnson, K.S., Gordon, R.M. and Coale, K.H., 1997. What controls dissolved iron concentrations in the world ocean? Marine Chemistry, 57: 137-161.

Johnson, C.M., Beard, B.L., Roden, E.E., Newman, D.K., and Nealson, K.H., 2004. Isotopic constraints on biogeochemical cycling of Fe. In: Geochemistry of non-traditional stable isotopes, Eds: Johnson, C.M., Beard, B.L., and Albarède, F., Reviews in Mineralogy & Geochemistry, 55: 359-408.

Jørgensen, B.B., 1977. Bacterial sulfate reduction within reduced microniches of oxidized marine sediments. Marine Biology, 41: 7-17.

Kester, D.R. and Pytkowicz, R.M., 1967. Determination of apparent dissociation constants of phosphoric acid in sea water. Limnology and Oceanography, 12: 243-252.

Kostka, J.E. and Luther, G.W. III, 1994. Partitioning and speciation of solid phase iron in saltmarsh sediments. Geochimica Cosmochimica Acta, 58: 1701-1710.

Kostka, J.E. and Nealson, K.H., 1995. Dissolution and reduction of magnetite by bacteria. Environmental Science and Technology, 29: 2535-2540.

Kostka, J.E., Stucki, J.W., Nealson, K.H. and Wu, J., 1996. Reduction of structural Fe(III) in smectite by a pure culture of *Shewanella putrefaciens* Strain MR-1. Clays and Clay Minerals, 44: 522-529.

König, I., Drodt, M., Suess, E., Trautwein, A.X., 1997. Iron reduction through the tan-green color transition in deep-sea sediments. Geochimica Cosmochimica Acta, 61: 1679-1683

Krauskopf, K.B., 1956. Factors controlling the concentration of thirteen trace metals in seawater. Geochimica Cosmochimica Acta, 12: 331-334.

Krom, M.D., Berner, R.A., 1980. Adsorption of phosphate in anoxic marine sediments. Limnology and Oceanography, 25: 797-806.

Kuma, K., Nishioka, J., Matsunaga, K., 1994. Controls of iron(III) hydroxide solubility in seawater: The influence of pH and natural organic chelators. Limnology and Oceanography, 41: 396-407.

Lear, P.R. and Stucki, J.W., 1989. Effects of iron oxidation state on the specific surface area of nontronite. Clays and Clay Minerals, 37: 547-552.

Leventhal, J. and Taylor, C., 1990. Comparison of methods to determine the degree of pyritisation. Geochimica Cosmochimica Acta, 54: 2621-2625.

Lord, C.J. III., 1980. The chemistry and cycling of iron, manganese, and sulfur in salt marsh sediments. Ph.D. thesis, University Delaware, 177 pp.

Lovley, D.R., 1987. Organic matter mineralization with the reduction of ferric iron: A review. Geomicrobiology Journal, 5: 375-399.

Lovley, D.R. and Phillips, E.J.P., 1988. Novel mode of microbial energy metabolism: Organic carbon oxidition coupled to dissimilatory reduction of iron and manganese. Applied and Environmental Microbiology, 54: 1472-1480

Lovley, D.R., 1991. Dissimilatory Fe(III) and Mn(IV) reduction. Microbiological Reviews 55: 259-287.

Lovley, D.R., 1997. Microbial Fe(III) reduction in subsurface environments. FEMS Microbiological Reviews, 20: 305-313.

Lovley, D.R., Coates, J.D., Saffarini, D. and Lonergan, D.J., 1997. Diversity of dissimilatory Fe(III)-reducing bacteria. In: Winkelman, G. and Carrano, C.J. (eds) Iron and Related Transition Metals in Microbial Metabolism, Harwood Academic Publishers, Switzerland, pp. 187-215.

Lyle, M., 1983, The brown-green color transition in marine sediments: A marker of the Fe(III)-Fe(II) redox boundary. Limnology and Oceanography, 28: 1026-1033.

Mackenzie, F.T. and Garrels, R.M., 1966, Chemical mass balance between rivers and oceans. American Journal of Science, 264: 507-525.

Martin, J.H., Gordon, R.M., Fitzwater, S.E., Broenkow, W.W., 1989. VERTEX: phytoplankton/iron studies in the Gulf of Alaska. Deep-Sea Research, 36: 649-680.

Martin, J.H., 1990. Glacial-interglacial CO_2 change: The iron hypothesis. Paleoceanography, 5: 1-13.

Martin, J.H., Gordon, R.M. and Fitzwater, S.E., 1991. The case for iron. In: Chisholm, S.W. and Morel, F.M.M. (eds). What controls phytoplankton production in nutrient-rich areas of the open sea?, ASLO Symposium, Lake San Marcos, California, Feb. 22-24, 1991, Allen Press, Lawrence.

Martin, J.H., Coale, K.H., Johnson, K.S. and Fitzwater, S.E., 1994. Testing the iron hypothesis in ecosystems of the equatorial Pacific Ocean. Nature, 371: 123-129.

Mayer, L.M., Jorgensen, J., Schnitker, D., 1991. Enhencement of diatom frustule dissolution by iron oxides. Marine Geology, 99: 263-266.

McAllister, C.D., Parsons, T.R. and Strickland, J.D.H., 1960. Primary productivity and fertility at station "P" in the north-east Pacific Ocean. Journal du Conseil, 25: 240-259.

McMurtry, G.M., Chung-Ho, W. and Hsueh-Wen, Y., 1983. Chemical and isotopic investigation into the origin of clay minerals from the Galapagos hydrothermal mound field. Geochimica Cosmochimica Acta, 47: 291-300.

Mehra, O.P. and Jackson, M.L., 1960. Iron oxide removal from soils and clays by a dithionite-citrate system buffered with sodium carbonate. Proceedings of the National Conference on Clays and Clay Mineralogy, 7: 317-327.

Michalopoulos, P. and Aller, R.C., 1995. Rapid clay mineral formation in Amazon delta sediments: Reverse weathering and oceanic cycles. Science, 270: 614-617.

Millero, F.J., Sotolongo, S. and Izaguirre, M., 1987. The oxidation kinetic of Fe(II) in seawater. Geochimica Cosmochimica Acta, 51: 793-801.

Morris, R.V., Lauer, H.V. Jr., Lawson, C.A., Gibson, E.K. Jr., Nace, G.A. and Stewart C., 1985. Spectral and other physicochemical properties of submicron powders of hematite (α-Fe_2O_3), maghemite (γ-Fe_2O_3), magnetite (Fe_3O_4), goethite (α-FeOOH), and lepidocrocite (γ-FeOOH). Journal of Geophysical Research, 90: 3126-3144.

Mortimer, R.J.G., Coleman, M.L., 1997. Microbial influence on the oxygen isotopic composition of diagenetic siderite. Geochimica Cosmochimica Acta, 61: 1705-1711.

Munch, J.C. and Ottow, J.C.G., 1980. Preferential reduction of amorphous to crystalline iron oxides by bacterial activity. Journal of Soil Science,129: 15-21.

Munch, J.C. and Ottow, J.C.G., 1982. Einfluß von Zellkontakt und Eisen(III)oxidform auf die bakterielle Eisenreduktion. Zeitschrift der Pflanzenernährung und Bodenkunde, 145: 66-77.

Murray, R.W. and Leinen, M., 1993, Chemical transport to the seafloor of the equatorial Pacific across a latitudinal transect at 135°W: Tracking sedimentary major, minor, and rare earth element fluxes at the equator and the inner tropical convergence zone. Geochimica Cosmochimica Acta, 57: 4141-4163.

Myers, C.R. and Nealson, K.H., 1988a. Bacterial manganese reduction and growth with manganese oxide as the sole electron acceptor. Science, 240: 1319-1321.

Myers, C.R. and Nealson, K.H., 1988b. Micorbial reduction of manganese oxides: Interactions with iron and sulfur. Geochimica Cosmochimica Acta, 52: 2727-2732.

Nittrouer, C.A., DeMaster, D.J., McKee, B.A., Cutshall, N.H., Larsen, I.L., 1983/1984. The effect of sediment mixing on Pb-210 accumulation rates for the Washington continental shelf. Marine Geology, 54: 201-221.

Norrish, K., Taylor, R.M., 1961. The isomorphous replacement of iron by aluminium in soil goethites. Journal of Soil Sciences, 12: 294-306.

Ottley, C.J., Davison, W., Edmunds, W.M., 1997. Chemical catalysis of nitrate reduction by iron(II). Geochimica Cosmochimica Acta, 61: 1819-1828.

Ottow, J.C.G., 1969. Der Einfluss von Nitrat, Chlorat, Sulfat, Eisenoxidform und Wachstumsbedingungen auf das Ausmass der bakteriellen Eisenreduktion. Zeitschrift der Pflanzenernährung und Bodenkunde, 124: 238-253.

Peiffer, S., Dos Santos Afonso, M., Wehrli, B. and Gächter, R., 1992. Kinetics and mechanism of the reaction of H_2S with lepidocrocite. Environmental Science and Technology, 26: 2408-2412.

Pena, F. and Torrent, J., 1984. Relationships between phosphate sorption and iron oxides in alfisols from a river terrace sequence of Mediterranean Spain. Geoderma, 33: 283-296.

Postma, D., 1982, Pyrite and siderite formation in brackish and freshwater swamp sediments. American Journal of Science, 282: 1151-1183.

Postma, D., 1985. Concentration of Mn and separation from Fe in sediments. Kinetics and stoichiometry of the reaction between birnessite and dissolved Fe(II) at 10°C. Geochimica Cosmochimica Acta, 49: 1023-1033.

Postma, D., Jakobsen, R., 1996, Redox zonation: Equilibrium constraints on the Fe(II)/SO4-reduction interface. Geochimica Cosmochimica Acta, 60: 3169-3175.

Poulton, S.W. and Raiswell, R., 2002, The low-temperature geochemical cycle of iron: from continental fluxes to marine sediment deposition. American Journal of Science, 302: 774-805.

Poulton, S.W., Krom, M.D., and Raiswell, R., 2004. A revised scheme for the reactivity of iron (oxyhydr)oxide minerals towards dissolved sulfide. Geochimica Cosmochimica Acta, 68: 3703-3715.

Prospero, J.M., 1981. Eolian transport to the world ocean. In: Emiliani, C. (ed), The sea, 7, Wiley, New York, pp. 801-874.

Prospero, J.M., Glaccum, R.A. and Nees, R.T., 1981. Atmospheric transport of soil dust from Africa to South America. Nature, 289: 570-572.

Pyzik, A.J. and Sommer, S.E., 1981, Sedimentary iron monosulfides: kinetics and mechanisms of formation. Geochimica Cosmochimica Acta, 45: 687-698.

Raiswell, R., Buckley, F., Berner, R.A. and Anderson, T.F., 1988. Degree of pyritisation as a paleoenvironmental indicator of bottom water oxygenation. Journal of Sedimentary Petrology, 58: 812-819.

Raiswell, R., Canfield, D.E. and Berner, R.A., 1994. A comparison of iron extraction methods for the determination of degree of pyritisation and the recognition of iron-limited pyrite formation. Chemical Geology, 111: 101-110.

Raiswell, R. and Canfield, D.E., 1996. Rates of reaction between silicate iron and dissolved sulfide in Peru Margin sediments. Geochimica Cosmochimica Acta, 60: 2777-2787.

Rijkenberg, M.J.A., Fischer, A.C., Kroon, J.J., Geringa, L.J.A., Timmermans, K.R., Wolterbeek, H.Th., and de Baar, H.J.W., 2005. The influence of UV irradiation on the photoreduction of iron in the Southern Ocean. Marine Chemistry, 93: 119-129.

Roden, E.E. and Zachara, J.M., 1996. Microbial reduction of crystalline iron(III) oxides: Influence of oxides surface area and potential for cell growth. Environmental Science and Technology, 30: 1618-1628.

Roden, E.E., and Wetzel, R.G., 2002. Kinetics of microbial Fe(III) oxide reduction in freshwater wetland sediments. Limnology Oceanography, 47: 198-211.

Roth, C.B. and Tullock, R.J., 1972. Deprotonation of nontronite resulting from chemical reduction of structural ferric iron. Proceedings of the International Clay Conference, Madrid, 89-98.

Rozenson, I. and Heller-Kallai, L., 1976a. Reduction and oxidation of Fe^{3+} in dioctahedral smectites - 1: Reduction with hydrazine and dithionite. Clays and Clay Minerals, 24: 271-282

Rozenson, I. and Heller-Kallai, L., 1976b. Reduction and oxidation of Fe^{3+} in dioctahedral smectites - 2: Reduction with sodium sulphide solutions. Clays and Clay Minerals, 24: 283-288.

Rue, E.L. and Bruland, K.W., 1995. Complexation of Fe(III) by natural organic ligands in the Central North Pacific as determined by a new competitive ligand equilibration/ adsorptive cathodic stripping voltammetric method. Marine Chemistry, 50: 117-138.

Ruttenberg, K.C., 1992. Development of a sequential extraction method for different forms of phosphorous in marine sediments. Limnology and Oceanography, 37: 1460-1482.

Schwertmann, U., 1964. Differenzierung der Eisenoxide des Bodens durch photochemische Extraktion mit saurer Ammoniumoxalat-Lösung. Zeitschrift zur Pflanzenernährung und Bodenkunde, 195: 194-202.

Schwertmann, U. Fitzpatrick, R.W., Taylor, R.M. and Lewis, D.G., 1979. The influence of aluminium on iron oxides. Part II. Preparation and properties of Al substituted hematites. Clays and Clay Minerals, 11: 189-200.

Schwertmann, U. and Murad, E., 1983. Effect of pH on the formation of goethite and hematite from ferrihydrite. Clays and Clay Minerals, 31:277-284.

Schwertmann, U. and Taylor, R.M., 1989. Iron oxides. In: Dinauer, R.C. (ed), Minerals in soil environments, Soil Science Society of America Book Series, 1, Madison, WI, pp. 379-438.

Schwertmann, U. and Cornell, R.M., 1991. Iron oxides in the laboratory. VCH Verlagsgesellschaft mbH, Weinheim, 137 pp.

Singer, A., Stoffers, P., Heller-Kallai, L. and Szafranek, D., 1984. Nontronite in a deep-sea ore from the south Pacific. Clays and Clay Minerals, 32: 375-383

Slomp, C.P., Van der Gaast, S.J., Van Raaphorst, W., 1996a. Phosphorus binding by poorly crystalline iron oxides in North Sea sediments. Marine Chemistry, 52: 55-73.

Slomp, C.P., Epping, E.H.G., Helder, W. and Van Raaphorst, W., 1996b, A key role for iron-bound phosphorus in authigenic apatite formation in North Atlantic continental platform sediments. Journal of Marine Research, 54: 1179-1205.

Sørensen, J. and Thorling, L., 1991, Stimulation by lepidocrocite (γ-FeOOH) of Fe(II)-dependent nitrite reduction. Geochimica Cosmochimica Acta, 55: 1289-1294.

Stookey, L.L., 1970, Ferrozine - A new spectrophotometric reagent for iron. Analytical Chemistry, 42: 779-781.

Stucki, J.W., 1981, The quantitative assay of minerals for Fe^{2+} and Fe^{3+} using 1,10-phenanthroline: II. A photochemical method. Soil Science Society of America Journal, 45: 638-641.

Stumm, W. and Morgan, J.J., 1996. Aquatic chemistry, 3rd edition, Wiley & Sons, London, 1022 pp.

Straub, K.L., Benz, M., Schinck, B., Widdel, F., 1996, Anaerobic, nitrate-dependent microbial oxidation of ferrous iron. Applied and Environmental Microbiology, 62: 1458-1460.

Sulzberger, B., Suter, D., Siffert, C., Banwart, S., Stumm, W., 1989. Dissolution of Fe(III) hydroxides in natural waters: Laboratory assessment on the kinetics controlled by surface coordination. Marine Chemistry, 28: 127-144.

Sundby, B., Silverberg, N., 1985. Manganese fluxes in the benthic boundary layer. Limnology and Oceanography, 30: 372-381.

Sundby, B., Anderson, L.G., Hall, P.O.J., Iverfeldt, Å, Rutgers van der Loeff, M., Westerlund, S.F.G., 1986. The effect of oxygen on release and uptake of cobalt, manganese, iron, and phosphate at the sediment-water interface. Geochimica Cosmochimica Acta, 50: 1281-1288.

Sundby, B., Gobeil, C., Silcerberg, N., Mucci, A., 1992. The phosphorus cycle in coastal marine sediments. Limnology and Oceanography, 37: 1129-1145.

Thamdrup, B., Glud, R.N. and Hansen, J.W., 1994. Manganese oxidation and in situ manganese fluxes from a coastal sediment. Geochimica Cosmochimica Acta, 58: 2563-2570.

Thamdrup, B. and Canfield, D.E., 1996. Pathways of carbon oxidation in continental margin sediments off central Chile. Limnology and Oceanography, 41: 1629-1650.

Torrent, J., Barrón, V. and Schwertmann, U., 1992, Fast and slow phosphate sorption by goethite-rich natural materials. Clays and Clay Mineralogy, 40: 14-21.

Trick, C.G., Andersen, R.J., Gillam, A. and Harrison, P.J., 1983. Prorocentrin: An extracellular siderophore produced by the marine dinoflagellate *Prorocentrum minimum*. Science, 219: 306-308.

Trick, C.G., 1989. Hydroxomate-siderophore production and utilization by marine eubacteria. Current Microbiology, 18: 375-378.

Uematsu, M., Duce, R.A., Prospero, J.M., Chen, L., Merrill, J.T., McDonald, R.L., 1983. Transport of mineral aerosol from Asia over the North Pacific

Ocean. Journal of Geophysical Research, 88: 5343-5352.

Van der Zee, C., Roberts, D.R., Rancourt, D.G., and Slomp, C.P., 2003. Nanogoethite is the dominant reactive oxyhydroxide phase in lake and marine sediments. Geology, 31: 993-996.

Van der Zee, C., Slomp, C.P., Rancourt, D.G., De Lange, G.J. and van Raaphorst, W., 2005. A Mössbauer spectroscopic study of the iron redox transition in eastern Mediterranean sediments. Geochimica Cosmochimica Acta, 69: 441-453.

Wallmann, K., Hennies, K., König, I., Petersen, W. and Knauth, H.-D., 1993. A new procedure for the determination of 'reactive' ferric iron and ferrous iron minerals in sediments. Limnology and Oceanography, 38: 1803-1812.

Wang, Y. and Van Capellen, P., 1996. A multicomponent reactive transport model of early diagenesis: Application to redox cycling in coastal sediments. Geochimica Cosmochimica Acta, 60: 2993-3014.

Wedepohl, K.H., 1995. The composition of the continental crust. Geochimica Cosmochimica Acta, 59: 1217-1232.

Wehrli, B., Friedel, G. and Manceau, A., 1995. Reaction rates and products of manganese oxidation at the sediment-water interface. In: Huang, C.P., O'Melia, C.R. and Morgan, J.J. (eds), Aquatic chemistry: Interfacial and interspecies processes, ACS Advances in Chemistry, 244, pp. 111-134.

Widdel, F., Schnell, S., Heising, S., Ehrenreich, A., Assmus, B. and Schink, B., 1993. Ferrous iron oxidation by anoxygenic phototrophic bacteria. Nature, 362: 834-835.

Wu, J. and Luther, G.W. III, 1995. Complexation of Fe(III) by natural organic ligands in the Northwest Atlantic Ocean by competitive ligand equilibration method and kinetic approach. Marine Chemistry, 50: 159-177.

Yeh, H.-W. and Savin, S.M., 1977. Mechanism of burial metamorphism of argillaceaous sediments: 3. O-isotope evidence. Bulletin of the Geological Society of America, 88: 1321-1330.

Zhuang, G., Duce, R.A. and Kester, D.A., 1990. The dissolution of atmospheric iron in surface seawater of the open ocean. Journal of Geophysical Research, 59: 16,207-16,216.

Zhuang, G. and Duce, R.A., 1993. The adsorption of dissolved iron on marine aerosol particles in surface waters of the open ocean. Deep Sea Research 40: 1413-1429.